People's Democratic Republic of Algeria
Ministry of Higher Education and
Scientific Research

University of Echahid Hamma Lakhdar - El Oued
Faculty of Science and Technology
Department of Electrical Engineering

Dissertation

ACADEMIC MASTER

Field: Wired and Wireless Telecommunication

Specialty: Telecommunication Systems

By: ZABI Imad & DJERIBIAI Oussama

SIMULATION STUDY OF FREE-SPACE OPTICAL COMMUNICATION SYSTEMS

Dissertation Submitted in Partial Fulfillment of the Requirements for the Master's Degree in Telecommunication Systems

Publicly defended on 28 May 2025

Board of Examiners:

Dr. BETKA Abir	**Chairman**
Dr. MADJOURI Abdel Kader	**Examiner**
Dr. HADJADJI Narimane	**Supervisor**

Academic Year: 2024/2025

بسم الله الرحمن الرحيم

Acknowledgments

First and foremost, I express my deepest gratitude to the Almighty for granting me the strength, wisdom, and perseverance to complete this journey of knowledge and growth. His divine guidance has been a source of inspiration and comfort throughout this endeavor.

I would like to extend my heartfelt appreciation to my supervisor, HADJADJI Narimane, for her unwavering support, invaluable guidance, and mentorship during the course of this project. Her expertise, encouragement, and constructive feedback have been instrumental in shaping my research and academic development.

To the faculty members, mentors, and all those who have contributed to my growth and learning, I offer my sincere thanks for their dedication and commitment to nurturing young minds and fostering a culture of academic excellence.

This project would not have been possible without the collective support and encouragement of all those who have touched my life in various ways. I am truly grateful for the opportunity to learn, grow, and contribute to the field of systems of wire-wireless telecommunication. Thank you all for being a part of this transformative

Dedication

I dedicate this humble work to:

To my father

To my mother

To my brothers

To my dear family, may God grant them health and long life

All my friends

To those who had a great impact on my life

Abstract

Abstract:

This study investigates the performance of Free-Space Optical (FSO) communication systems through simulations conducted using OptiSystem software. FSO technology, employing light beams for wireless data transmission, offers high-bandwidth and secure communication without physical infrastructure. The research specifically examines a system utilizing 16-Quadrature Amplitude Modulation (16-QAM) at a 10 Gb/s data rate. Performance analysis is carried out under various atmospheric conditions prevalent in El-Oued, Algeria, including clear weather, fog, rain, and dust storms.

The study evaluates three common FSO wavelengths: 850 nm, 1310 nm, and 1550 nm, assessing key performance indicators such as Q-factor and Bit Error Rate (BER) to determine signal quality and system reliability. Simulation results reveal that the 1550 nm wavelength exhibits superior performance, maintaining robust signal integrity and minimal error rates even under moderate weather impairments. In contrast, the 850 nm and 1310 nm wavelengths demonstrate significant degradation in the presence of fog and dust.

The findings of this research suggest that the 1550 nm wavelength is the most appropriate for FSO deployment in arid environments like El-Oued. Furthermore, the study indicates the potential of employing techniques such as spatial diversity or adaptive modulation to enhance the overall reliability of FSO systems in such challenging climatic conditions.
Keywords: Free-Space Optical (FSO) Communication,16-QAM Modulation, Bit Error Rate (BER), Q-Factor, Atmospheric Attenuation, Optical Coherence System

الملخص:

تستعرض هذه الدراسة أداء أنظمة الاتصالات البصرية في الفراغ من خلال محاكاة أجريت باستخدام برنامج OptiSystem. تعتمد تقنية الاتصال البصري في الفراغ على حزم ضوئية لنقل البيانات لاسلكيًا، مما يُتيح اتصالات عالية النطاق الترددي وآمنة دون الحاجة إلى بنية تحتية مادية. تتناول البحوث نظامًا يستخدم تقنية QAM-16 تعديل الاتساع الرباعي بسرعة نقل بيانات قدرها 10 جيجابت/ثانية. يتم تحليل الأداء في ظل ظروف جوية متعددة سائدة في ولاية الوادي بالجزائر، تشمل الأجواء الصافية والضباب والأمطار وعواصف الغبار.

تقيّم الدراسة ثلاث أطوال موجية شائعة في نظم الاتصال البصري في الفراغ:850 نانومتر، 1310 نانومتر، و1550 نانومتر، مع التركيز على مؤشري الأداء الرئيسيين، وهما عامل الجودة ومعدل خطأ البتات، لتحديد جودة الإشارة وموثوقية النظام.
أظهرت نتائج المحاكاة تفوق الطول الموجي 1550 نانومتر من حيث الحفاظ على سلامة الإشارة وانخفاض معدل الأخطاء حتى في ظل الاضطرابات الجوية المتوسطة. على النقيض من ذلك، سجلت الأطوال الموجية 850 نانومتر و1310 نانومتر تدهورًا ملحوظًا في الأداء عند وجود الضباب والغبار.

تشير نتائج هذه الدراسة إلى أن الطول الموجي 1550 نانومتر هو الأنسب لنشر نظم الاتصال البصري في الفراغ في البيئات القاحلة مثل الوادي. كما تبرز الدراسة إمكانية استخدام تقنيات مثل التنوع المكاني أو التعديل التكيفي لتحسين الموثوقية الإجمالية لهذه النظم في مثل هذه الظروف المناخية الصعبة.
الكلمات الرئيسية: الاتصال البصري في الفضاء الحر، 16-تعديل السعة الرباعي، معدل خطأ البتات، عامل الجودة، التوهين الجوي، نظام التماسك البصري.

Résumé :

Cette étude examine les performances des systèmes de communication optique en espace libre (FSO) au moyen de simulations réalisées avec le logiciel OptiSystem. La technologie FSO, qui utilise des faisceaux lumineux pour la transmission de données sans fil, offre une bande passante élevée et une sécurité accrue sans nécessiter d'infrastructure physique. La recherche porte spécifiquement sur un système employant une modulation d'amplitude en quadrature 16 (16-QAM) à un débit de 10 Gb/s.

L'analyse des performances est conduite sous diverses conditions atmosphériques typiques d'El-Oued, en Algérie : ciel clair, brouillard, pluie et tempêtes de poussière. Trois longueurs d'onde couramment utilisées en FSO :850 nm, 1310 nm et 1550 nm sont évaluées à l'aide d'indicateurs clés tels que le qualité facteur (Q-factor) et le taux d'erreur binaire (TEB), afin d'estimer la qualité du signal et la fiabilité du système.

Les résultats de simulation montrent que la longueur d'onde de 1550 nm présente la meilleure performance, en maintenant une intégrité de signal robuste et un taux d'erreur minimal même en cas de perturbations atmosphériques modérées. En revanche, les longueurs d'onde de 850 nm et 1310 nm subissent une dégradation notable des performances en présence de brouillard et de poussière.

Les conclusions de cette étude recommandent l'utilisation de la longueur d'onde 1550 nm pour le déploiement de systèmes FSO dans les environnements arides tels qu'El-Oued. En outre, le recours à des techniques telles que la diversité spatiale ou la modulation adaptative pourrait renforcer davantage la fiabilité globale de ces systèmes dans des conditions climatiques difficiles.

Mots clés : Communication optique en espace libre, Modulation 16-QAM, Taux d'erreur binaire (TEB), Facteur Q, Atténuation atmosphérique, Système de cohérence optique.

Contents

Contents

List of Figures

List of Tables

List of Abbreviations

FSO	Free-Space Optical
LED	Light-Emitting Diode
MIMO	Multiple-Input Multiple-Output
UAV	Unmanned Aerial Vehicle
RF	Radio Frequency
LOS	Line-of-Sight
NLOS	Non-Line-of-Sight
LEO-LEO	Inter-Low-Earth Orbit
LEO-GEO	Intra-Orbital (Low-Earth Orbit to Geostationary Earth Orbit)
DSL	Digital Subscriber Line
Li-Fi	Light Fidelity
FEC	Forward Error Correction
PRBS	Pseudo-Random Bit Sequence
ISI	Inter-Symbol Interference
DB	Duobinary
RZ	Return to Zero
CSRZ	Carrier-Suppressed Return to Zero
Laser	Light Amplification by Stimulated Emission of Radiation
IM	Intensity Modulation
OOK	On-Off Keying
PPM	Pulse Position Modulation
DD	Direct Detection
MZM	Mach-Zehnder Modulator
PSK	Phase Shift Keying
BPSK	Binary Phase Shift Keying
QPSK	Quadrature Phase Shift Keying
QAM	Quadrature Amplitude Modulation
OFDM	Orthogonal Frequency Division Multiplexing
ACO-OFDM	Asymmetrically Clipped Optical OFDM
DCO-OFDM	DC-biased Optical OFDM
DSP	Digital Signal Processing
IFFT	Inverse Fast Fourier Transform
OA	Optical Amplifier

EDFA	Erbium-Doped Fiber Amplifier
SOA	Semiconductor Optical Amplifier
ASE	Amplified Spontaneous Emission
SNR	Signal-to-Noise Ratio
WDM	Wavelength Division Multiplexing
RoFSO	Radio over Free-Space Optics
PIN	Positive-Intrinsic-Negative (Diode)
APD	Avalanche Photodiode
BER	Bit Error Rate
Q Factor	Quality Factor
AGC	Automatic Gain Control

General Introduction

General Introduction

Free-space optical (FSO) communication is an emerging wireless technology that conveys data by transmitting modulated light beams typically from lasers or LEDs through the atmosphere rather than through fiber or copper conductors. Unlike guided optical fibers, FSO links are "unguided," offering rapid deployment, license-free operation, immunity to electromagnetic interference, and very high bandwidth with minimal latency. These attributes make FSO particularly attractive for applications ranging from last-mile enterprise and cellular backhaul to secure satellite-to-ground and inter-satellite links.

In desert environments like El Oued region in Algeria, weather conditions such as light fog (~18 dB/km) and severe dust storms (>50 dB/km) pose particularly harsh attenuation challenges. Understanding these impairments is crucial for designing robust FSO links that meet stringent reliability targets (bit error rate (BER) $< 10^{-9}$, Q factor > 6) under real-world conditions.

This thesis addresses these challenges by modeling El Oued's atmospheric impairments in OptiSystem, simulating a 10 Gb/s 16-QAM FSO link at key wavelengths (850 nm, 1310 nm, 1550 nm), and evaluating performance metrics such as bit error rate, Q factor, and eye diagrams across various representative weather scenarios. Through this work, we aim to identify the optimal wavelength and system configurations for reliable, high-capacity FSO deployment in arid, dust-prone regions.

- **Chapter 1** Covers FSO architecture, components (transmitter, receiver, 16-QAM/coherent detection), and key metrics (BER, Q-factor, SNR), plus the main atmospheric impairments (absorption, scattering, turbulence).
- **Chapter 2** Lays out the key design aspects of FSO systems, including optimal wavelength choices (850 nm and 1550 nm), beam optics, and major atmospheric effects like absorption, scattering, turbulence, and weather-related attenuation, along with techniques such as beam expansion and diversity methods to improve link reliability and performance.
- **Chapter 3** Simulates a 10 Gb/s 16 QAM free-space optical link over seven meteorological conditions with varying transmission distances. The system's performance is assessed by bit error rate values, Q factor, and eye diagrams, and identifies the ideal wavelength and configurations for dependable, high-capacity desert deployment.

This thesis summarizes the key findings highlighting the wavelength and design choices that best overcome arid and dust-laden conditions and discusses their implications for deploying next-generation, high-capacity FSO networks in harsh desert climates.

Chapter I:

Fundamentals of Free Space Optics

I.1 Introduction

I.1.1 Optical communication and its advantages

Optical communication is a method that conveys signals via light rather than electrical currents, via optical fibers. It comprises essential components, including a transmitter, receiver, modulator, demodulator, transparent channel, and optical signals. Optical communication systems are categorized as guided systems, which contain the beam (optical fiber), and unguided systems, where the beam disperses in space.

Free-space optical (FSO) communication, an unguided optical system, facilitates data transmission via open air utilizing laser or Light-Emitting Diodes (LED) beams instead of fiber-optic cables. It has numerous benefits, including elevated bandwidth, minimal latency, and resistance to electromagnetic interference, rendering it a compelling option for diverse applications such as satellite communications, deep-space exploration, and terrestrial wireless networks.

In contrast to fiber-optic communication, which necessitates physical infrastructure, Free Space Optics (FSO) provides flexibility and swift deployment, rendering it especially advantageous in distant or urban locales where cable installation is problematic. Nonetheless, its performance may be compromised by meteorological circumstances such as fog, precipitation, and turbulence, which can diminish signal quality and reliability. Notwithstanding these obstacles, progress in adaptive optics, error correction methodologies, and hybrid communication frameworks is perpetually enhancing the efficacy of FSO systems. With the increasing demand for high-speed and secure communication, free-space optical communication emerges as a viable alternative to traditional wired and wireless technologies.

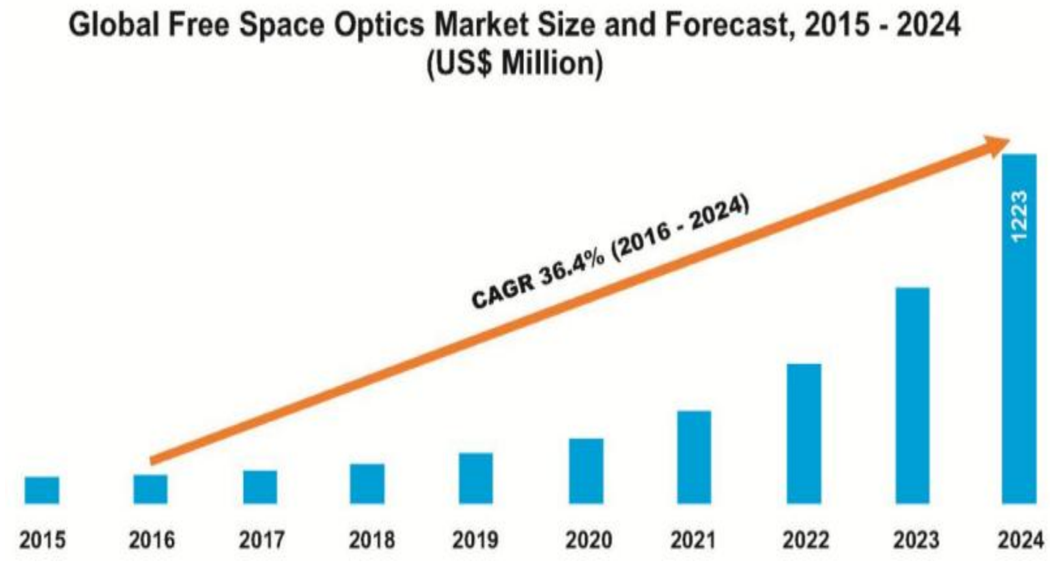

Figure I.1: *Prediction of the growth of FSO technology.[1]*

I.1.2 History and Development of Free Space Optical (FSO) Communication

Free Space Optical (FSO) communication has evolved significantly since its conceptual origins in the 19th century. The earliest demonstration dates to 1880 when Alexander Graham Bell invented the Photophone, which transmitted voice signals using modulated sunlight. However, the lack of reliable light sources and detectors limited progress until the invention of the laser in 1960, which provided a stable and coherent beam for optical transmission. Throughout the 1970s and 1980s, FSO gained traction in military and space applications, with organizations like NASA and DARPA exploring its potential for secure satellite communications due to its resistance to interception. By the 1990s, advancements in laser and detector technologies enabled more practical implementations, leading to its adoption in high-speed, low-latency data links for defense and aerospace.

The early 2000s marked the beginning of commercial FSO systems, with companies like LightPoint and fSONA developing solutions for enterprise and telecom backhaul, particularly in urban areas where fiber deployment was costly. Despite challenges like atmospheric attenuation (fog, rain), innovations in adaptive optics, MIMO techniques, and high-power lasers improved reliability. In the 2010s, FSO found applications in 5G backhaul, disaster recovery networks, and unmanned aerial vehicle (UAV) communications. Today, FSO is a key technology for satellite constellations (e.g., SpaceX's Starlink laser links) and is being tested for deep-space communication (e.g., NASA's LCRD mission). Future advancements include quantum-secured FSO, hybrid RF/FSO systems, and integration with next-gen wireless networks, reinforcing its role as a high-bandwidth, secure, and scalable alternative to traditional wireless and fiber-optic communications.[2]

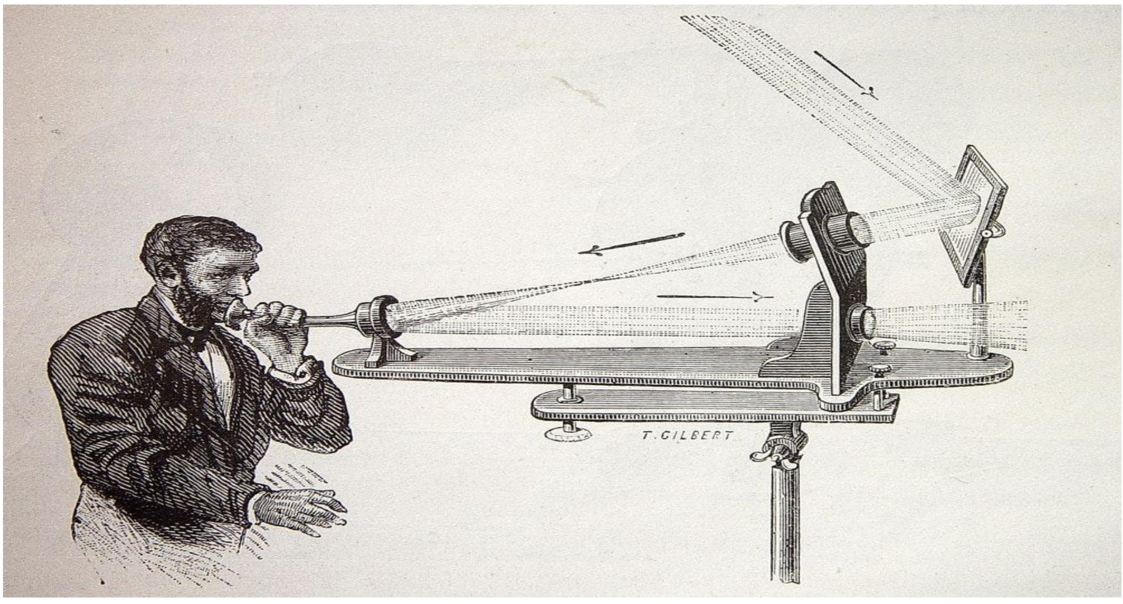

Figure I.2: *Bell's demonstration of the "photophone" in 1880. [3]*

I.1.3 FSO Communication System

FSO, or Free Space Optics, is a line-of-sight technology utilizing lasers to establish optical bandwidth connections. It is an optical communication method that transmits light through free space, such as air, outer space, or vacuum, enabling wireless data transmission for telecommunications and computer networking. Currently, FSO can achieve data rates of up to 2.5 Gbps for voice, data, and video communications without the need for optical fiber cables or securing spectrum licenses [4]. It operates within the 780-1600 nm wavelength range and incorporates optical/electrical (O/E) and electrical/optical (E/O) converters.

FSO technology requires a light source, which can be lasers (light amplification by stimulated emission of radiation). While the foundational concept of using lasers is like optical fiber transmission, the primary distinction lies in the transmission medium, light travels faster through air than through glass, supporting the classification of FSO as optical communications operating at the speed of light. This technology serves as an alternative to line-of-sight (LOS) radio relay communication systems [5].

FSO systems are also known as open-air photonics, free-space photonics, optical wireless technology, or infrared broadband technology. They operate in the near-infrared spectrum, with wavelengths ranging from 399-352.6 THz to 199.8-187.3 THz. Their communication method is like fiber optics, but instead uses a pair of photodetector transceivers connected via a laser beam in free space. These line-of-sight optical links offer significant potential for high-capacity data transmission and seamless connectivity [6][7].

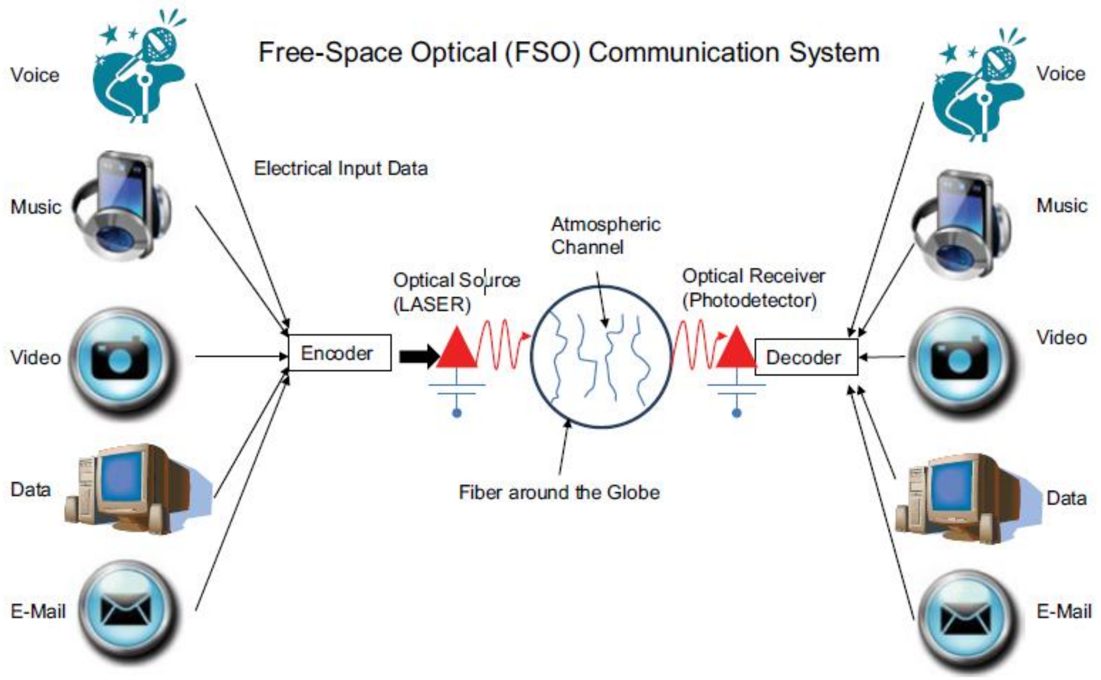

Figure I.3: *A scheme of FSO communication technology with optical wireless and different user connectivity.[8]*

Three key components of FSO include a transmitter that sends optical radiation while adhering to Beer-Lambert's law, a free-space transmission channel affected by environmental factors such as clouds, rain, smoke, gases, temperature variations, fog, and aerosols, and a receiver that processes the incoming signal. Typical communication links range from 300 m to 5 km, with the potential for longer distances (8–11 km) based on speed and required availability [5].

I.1.4 Applications of FSO Communication Systems

Applications of FSO communication systems span from short-range (<1 km) applications to long-range and space applications. This technology offers a broadband solution, providing high data rates without the need for cabling, which is ideal for connecting end users to the backbone. Short-range applications enable last-mile access by linking various towers and buildings in urban settings where digging trenches for cables is impractical. The system can facilitate point-to-point, point-to-multipoint, and broadband links. Here are several noteworthy applications of FSO systems [9]:

- **Enterprise Connectivity:** FSO links are easily deployable and can connect multiple towers and buildings, creating local area connectivity. They can also link metropolitan area fiber rings, support new network connections.
- **Fiber Backup:** In the event of an optical fiber link failure, FSO links can serve as backup connections, ensuring system availability.
- **Point-to-Point Links:** This includes inter-low-Earth orbit (LEO-LEO) and intra-orbital (low-Earth orbit-geostationary Earth orbit (LEO-GEO)) links, as well as satellite-to-ground and ground-to-satellite connections. Such links necessitate robust pointing and tracking systems, and factors like transmitter output power, power consumption, size, mass, and deployment costs tend to increase with the link range.
- **Point-to-Multipoint Links:** Unique applications of FSO systems also encompass multi-platform multi-static sensing, interoperable satellite communications, and shared spaceborne processing.
- **Hybrid Wireless Connection/Network Redundancy:** Given that FSO communication is susceptible to adverse weather like fog and heavy snow, combining FSO links with microwave links known for operating at high frequencies in the GHz range. This can help achieve 100% network availability while offering comparable data rates.
- **Disaster Recovery:** FSO communication systems provide scalable, high-capacity links during instances of existing network collapses, ensuring resilience.
- **Backhaul for Cellular Networks:** With the increased demand for broadband connectivity in 3G/4G networks, there is a pressing need to enhance backhaul capacity between cellular

towers. While deploying fiber-optic cables can be labor-intensive and expensive, FSO communication systems present a valuable alternative for providing necessary backhaul support [9].

I.1.5 Comparison of FSO with other technologies (fiber optics, microwave, radio frequency):

I.1.5.a Free Space Optics (FSO) Against Fiber Optics

FSO is quick and cost-effective to implement since it does not require physical infrastructure. However, fiber optics offers superior reliability and supports extremely high data rates (up to terabits per second) with minimal signal loss over long distances. FSO's performance can be negatively impacted by weather conditions such as fog and rain.

I.1.5.b FSO Against Microwave Communication

FSO provides higher bandwidth and data rates without experiencing electromagnetic interference. In contrast, microwave signals can cover longer distances and are less affected by weather, making them more reliable for long-range communication. While FSO requires a clear line of sight, microwave links can overcome some obstacles and perform better in adverse weather conditions.

I.1.5.c FSO Against Radio Frequency (RF) Communication

FSO operates within an unlicensed spectrum, allowing it to avoid the regulatory challenges and interference often faced by RF systems. Additionally, FSO signals do not penetrate walls, enhancing security. However, RF communication excels in non-line-of-sight situations and can cover greater distances, making it more suitable in obstructed environments.

I.1.5.d FSO Against Wired Communication (Copper Cables/DSL)

FSO delivers significantly higher data rates without the need for expensive cables. On the other hand, wired systems ensure consistent performance regardless of weather conditions and do not require a clear line of sight, which makes them more reliable for fixed installations. FSO is ideal for scenarios that demand rapid deployment and high-speed connectivity.

I.1.5.e FSO Against Li-Fi (Light Fidelity)

FSO and Li-Fi both utilize light for communication, but they serve different environments. FSO is designed for outdoor point-to-point links over long distances, whereas Li-Fi is optimized for indoor wireless communication, often within a room. FSO offers greater range and higher power, while Li-Fi enables data transmission through LED lighting and provides high-speed, secure, and interference-free connectivity indoors. However, both systems require a line of sight and are sensitive to physical obstructions.

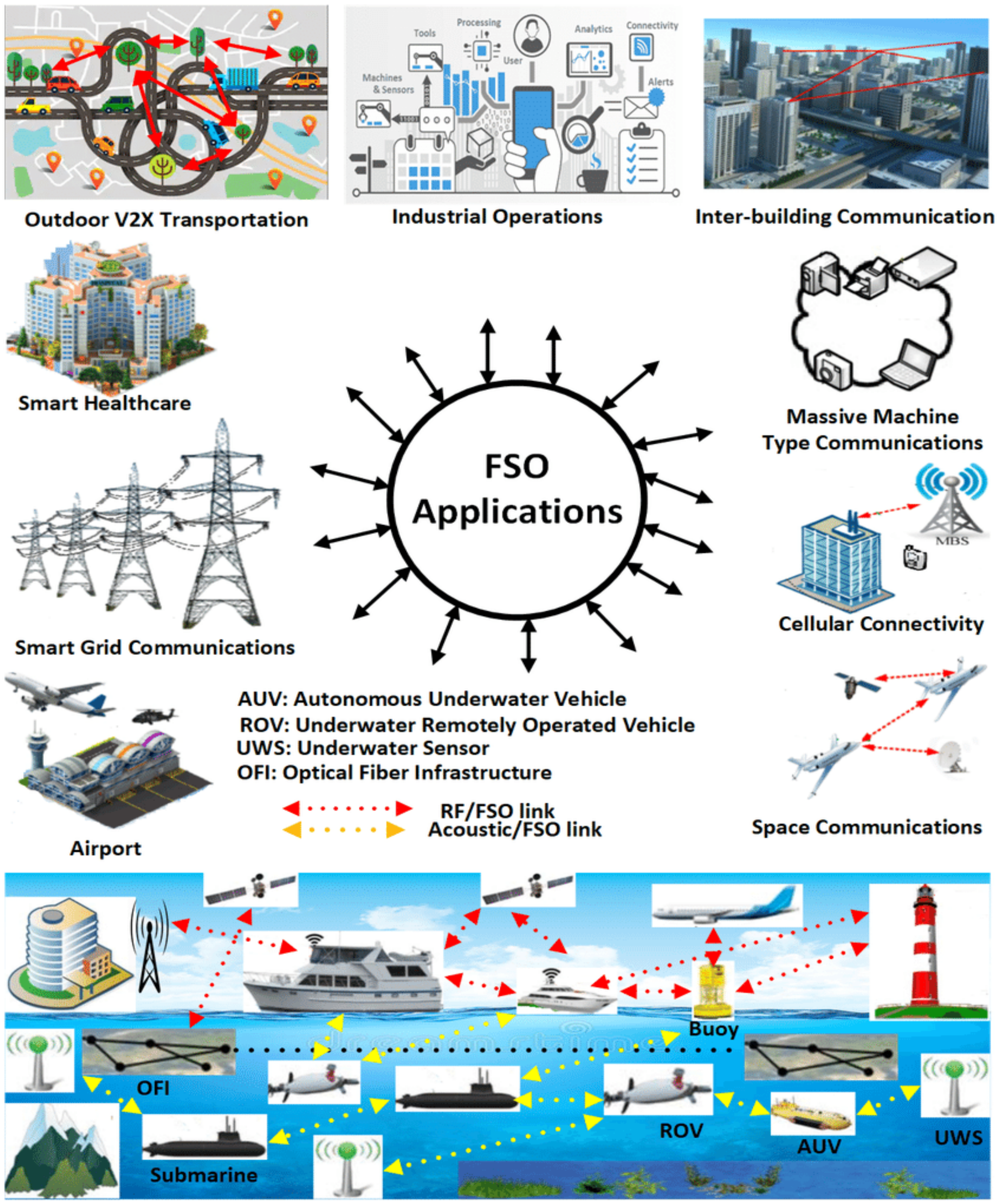

Figure I.4: *A few applications of FSO systems connectivity. [10]*

I.2 Basic components of FSO communication systems

The components of Free Space Optics (FSO) consist of three stages: the transmitter, which employs Beer-Lambert's law to emit optical radiation through the atmosphere; the free space transmission channel, characterized by turbulent disturbances such as clouds, rain, smoke, gases, temperature variations, fog, and aerosols; and the receiver, which interprets the incoming signal. While distances of 8-11 km may be utilized based on speed and required availability, most connections range from 300 m to 5 km. This section is essential as it offers a systematic introduction to the FSO methodology. [11]

I.2.1 Transmitter

A sequence of binary elements is generated from the information transmitted by the source. The quantity of binary elements transmitted during a specified duration, expressed in bits per second, is referred to as the bit rate D. To rectify errors, thereafter, incorporate the redundancy bits of the forward error correction (FEC) codes into the binary sequence to encode the information bits.

The subsequent step involves generating a time-domain digital waveform by correlating these bits to designated symbols. A symbol can encode one or several bits, contingent upon the modulation type. Finally, for the data to traverse the transmission channel during the optical modulation phase, it must be inscribed onto a carrier. [11]

I.2.2 Bit sequence

Coherent optical systems necessitate bit sequences for the transmission of digital information. These sequences, often termed multiple-bits-per-symbol or pseudo-random bit sequences (PRBS), enhance spectral efficiency and data rates. They are established with a specified duration and bit rate, representing the data information. Phase noise and inter-symbol interference (ISI) are mitigated by PRBS. They are essential for the receiver's error-correcting procedure as they provide accurate data recognition and decoding transmission. [12]

I.2.3 Generation of electrical signals

The first step in creating electrical signals is to encode the data into binary digits (0s and 1s); the bits are then converted into the symbols of the modulation format. An oversampled representation with the same information is produced by the independent and symmetrical distribution of the symbol sequence to the pulse's form.[13][14]

$$u_E(t) = \sum_{\infty}^{\infty} S_k g(t) kT_s \tag{I.1}$$

The pulse shaping filter regulates the bandwidth of the resulting signal, where g(t) is the pulse form, kT_s is the instantaneous symbol, and s_k is the symbol.

The theoretical analysis of optical transmission can consider a variety of optical pulse forms, such as Duobinary (DB), Nyquist, Return to Zero (RZ), and Carrier Suppressed Return to Zero (CSRZ). These pulse forms are used in many optical devices and are essential for modifying optical signals to transport data. [14]

I.2.4 The laser

A laser (Light Amplification by Stimulated Emission of Radiation, often a diode laser) that constantly produces light at a particular wavelength and power is the transmitter's primary component. Although the power of a light signal is measured in milliwatts (mW), decibels-milliwatts (dBm) are the most used unit in practical applications. [14]

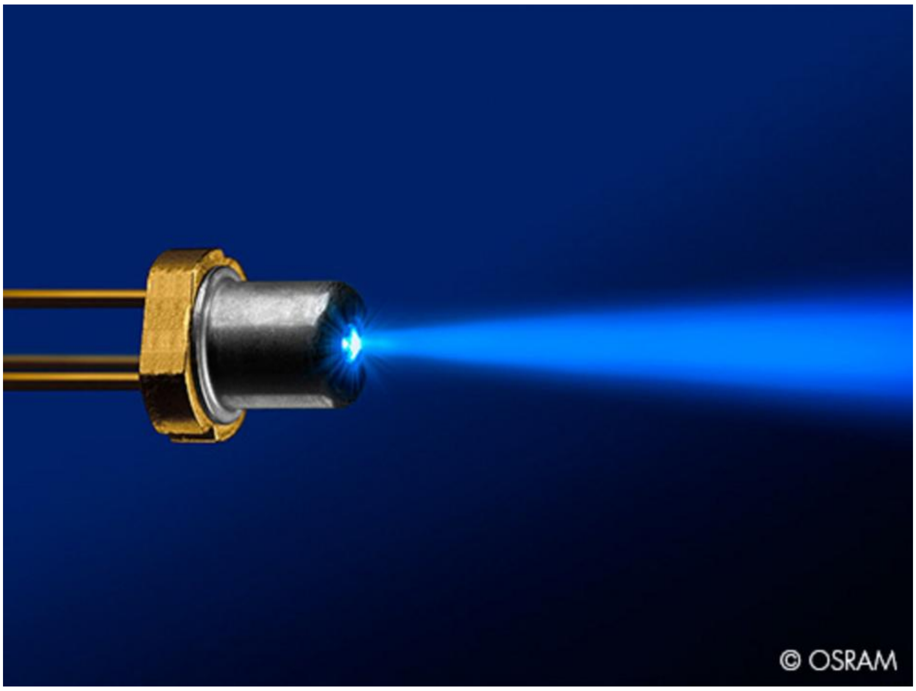

Figure I.5: *Scheme of a laser diode. [15]*

I.2.5 Modulation techniques used in FSO system

I.2.5.a Intensity Modulation (IM)

In FSO systems, Intensity Modulation is implemented by directly varying the optical power of the light source (laser/LED) to encode data. The modulator in the transmitter typically consists of a driver circuit that converts electrical data signals into corresponding optical intensity variations. Common IM techniques include On-Off Keying (OOK), where the light source is switched on (logic '1') or off (logic '0'), and Pulse Position Modulation (PPM), where data is encoded in the position of a pulse within a symbol period. The modulator must ensure precise control over the light intensity to maintain signal integrity, often requiring bias control circuits to avoid nonlinear distortions. Since IM does not use phase or frequency modulation, the transmitter design remains simple, making it cost-effective for short-range FSO links [16]. IM/DD systems are particularly vulnerable to atmospheric turbulence, scintillation, and attenuation, as these directly impact the received signal intensity [17].

I.2.5.b Coherent Modulation techniques

In coherent FSO systems, the transmitter employs phase and amplitude modulators (e.g., Mach-Zehnder Modulators, MZMs) to encode data onto the optical carrier using PSK (BPSK/QPSK) or QAM (16-QAM, 64-QAM). Unlike IM, coherent modulation preserves phase information, requiring a stable laser source and precise modulator control to minimize phase noise. The modulator typically integrates IQ mixers to generate in-phase (I) and quadrature (Q) components, enabling complex modulation formats. Since coherent detection is sensitive to atmospheric phase distortions, the transmitter may incorporate pilot tones or digital pre-distortion to compensate for turbulence effects. While offering superior spectral efficiency, coherent modulators are more complex and power-intensive than IM-based transmitters, limiting their use to high-performance FSO applications.

QAM modulation formats perform better than CS-RZ (Carrier-Suppressed Return-to-Zero) under medium-turbulence atmospheric scintillation [18].

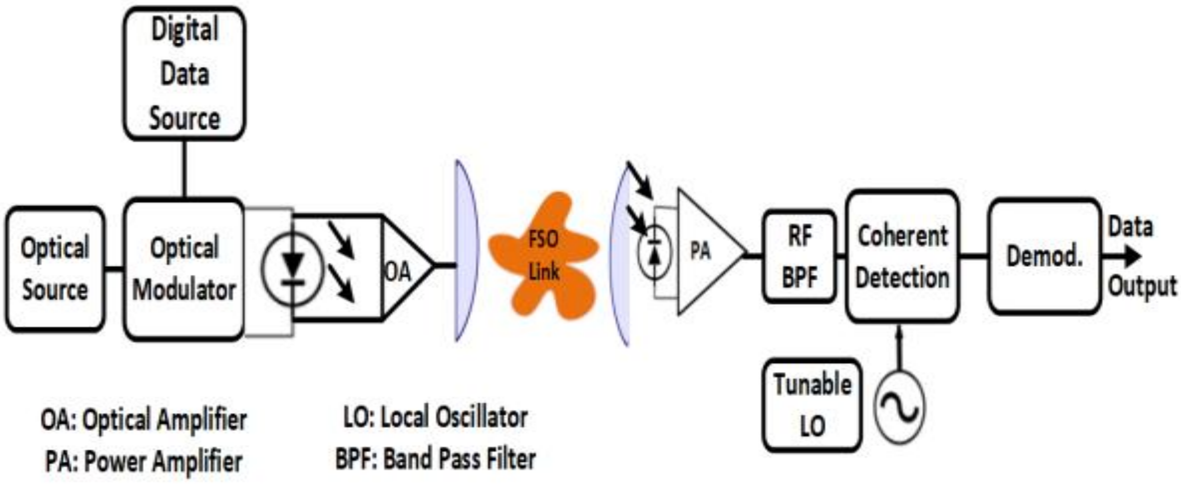

Figure I.6: *Coherent Detection in FSO Systems.*

I.2.5.c Advanced Modulation Schemes for Turbulence Mitigation

To counteract atmospheric turbulence, advanced modulation schemes like Orthogonal Frequency Division Multiplexing (OFDM) and adaptive modulation are employed in the transmitter. In Optical OFDM (O-OFDM), the modulator splits the incoming data stream into multiple subcarriers, each modulated using Quadrature Amplitude Modulation (QAM) or Phase-Shift Keying (PSK) before being converted to an intensity signal via Hermitian symmetry (for ACO-OFDM) or DC biasing (for DCO-OFDM). Adaptive modulation dynamically adjusts the modulation order (e.g., switching between OOK and 16-QAM) based on real-time channel feedback. The modulator in these schemes requires digital signal processing (DSP) blocks, including inverse Fast Fourier Transform (IFFT) and cyclic prefix insertion, increasing complexity but improving robustness against fading.

I.3 Optical Amplifiers

Optical amplifiers (OAs) are key components for compensating signal attenuation, extending range, and improving receiver sensitivity in FSO systems. They operate by directly amplifying optical signals, enabling long-haul and multi-hop transmissions while overcoming power limitations and thermal noise. The two primary types are Erbium-Doped Fiber Amplifiers (EDFAs), preferred for their 1550 nm bandwidth in WDM systems, and Semiconductor Optical Amplifiers (SOAs), which help mitigate turbulence-induced scintillation.

However, OAs introduce amplified spontaneous emission (ASE) noise, degrading the signal-to-noise ratio. This noise can be partially controlled using optical bandpass filters before detection. While OAs enhance performance in WDM and RoFSO applications, their ASE noise limits compatibility with avalanche photodiodes, presenting a key design challenge for optimal FSO system implementation. [19][20]

I.4 Receiver Systems

Free Space Optical communication systems employ two distinct receiver architectures: direct detection and coherent detection, each offering unique advantages and trade-offs in system performance and implementation complexity.

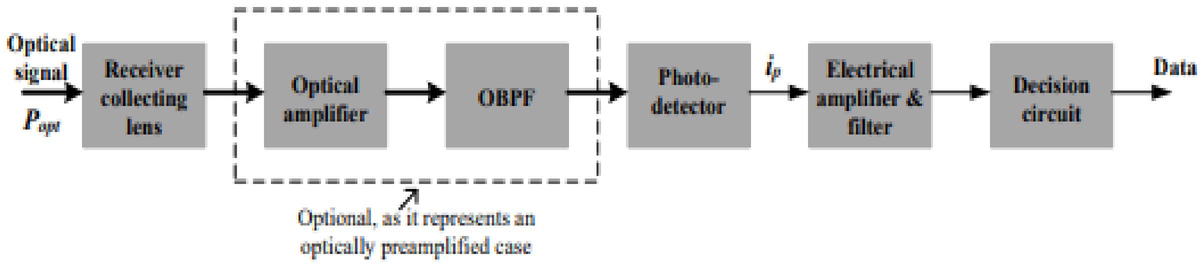

Figure I.7: *Block diagram of a typical FSO receiver.*

I.4.1 Direct detection receivers

Represent the predominant approach in practical FSO systems due to their relative simplicity and cost-effectiveness. These systems operate by measuring the intensity of the received optical signal using photodetectors such as PIN diodes or avalanche photodiodes (APDs). The receiver architecture typically includes an optical front-end with collecting optics and bandpass filters, followed by a transimpedance amplifier and clock recovery circuits. While direct detection offers implementation advantages, it is fundamentally limited to intensity modulation schemes and suffers from sensitivity constraints imposed by shot noise and thermal noise. Modern direct detection systems employ advanced techniques such as optical preamplification, adaptive thresholding, and spatial diversity to mitigate atmospheric turbulence effects and improve performance. [21][22]

I.4.2 Coherent detection receivers

Provide superior sensitivity and spectral efficiency by preserving both the amplitude and phase information of the optical field. These systems utilize a local oscillator laser combined with optical hybrids to enable detection of advanced modulation formats including phase-shift keying (PSK) and quadrature amplitude modulation (QAM).

The coherent receiver architecture requires precise phase matching between the signal and local oscillator, along with sophisticated digital signal processing for carrier recovery and phase estimation. While offering 3-6 dB sensitivity improvement over direct detection, coherent systems face significant implementation challenges in FSO environments, including phase noise induced by atmospheric turbulence and stringent alignment requirements.

Recent advances in digital coherent technology and adaptive optics have made coherent detection increasingly viable for high-capacity FSO links, particularly in space communication applications where its sensitivity advantages are most valuable. [23][24].

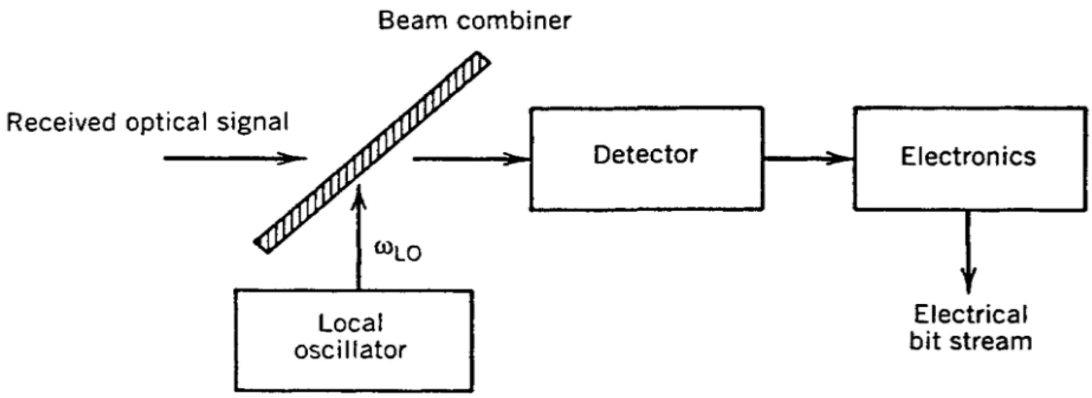

Figure I.8: *Diagram of a Coherent detection scheme.*

In Free Space Optics (FSO), choosing between direct and coherent detection involves balancing performance and complexity. Direct detection, which measures signal intensity, is commonly used in terrestrial links due to its simplicity and cost-effectiveness.

Coherent detection, while more complex and costly, offers higher sensitivity and spectral efficiency by capturing both amplitude and phase. It is suited for advanced applications like satellite and quantum communication.

Hybrid systems that merge both methods are emerging, aiming to optimize performance without excessive complexity. The choice depends on specific requirements such as cost, range, and data rate.

I.5 Performance Metrics for FSO Systems

The performance of Free Space Optical communication systems is evaluated through several key metrics that quantify link reliability, signal quality, and transmission efficiency. These metrics are critical for system design, optimization, and comparison with alternative communication technologies.

I.5.1 The Bit Error Rate (BER)

The BER measures the probability of incorrect bit detection at the receiver and serves as a fundamental indicator of signal integrity. FSO systems typically target BER values below 10^{-9} for high-quality communication, though atmospheric turbulence, misalignment, and background noise can significantly degrade performance. In other words, it is the ratio of the number of erroneous bits to the total number of transmitted bits [25]:

$$\text{BER} = \frac{\text{Number of Erroneous Bits}}{\text{Total Number of Transmitted Bits}} \tag{I.2}$$

BER is influenced by modulation scheme, receiver sensitivity, and channel conditions, with coherent detection often achieving lower BER than direct detection under similar conditions.

I.5.2 Q Factor

The Quality Factor (Q) provides a measure of the signal quality at the receiver by quantifying how distinctly the binary '1's and '0's are separated in the presence of noise. It is defined as the difference between the mean levels for logical '1' and '0', divided by the sum of the noise standard deviations associated with these levels:

$$Q = \frac{v_1 - v_0}{\sigma_1 + \sigma_0} \tag{I.3}$$

Here, v_1 and v_0 are the average signal levels for a binary '1' and a binary '0', respectively, while σ_1 and σ_0 represent the noise standard deviations around these levels. Under the assumption that the noise follows a Gaussian distribution, the relationship between BER and Q Factor is given by [26]:

$$\text{BER} = \frac{1}{2}\, erfc\left(\frac{Q}{\sqrt{2}}\right) \tag{I.4}$$

This equation links the measurable Q Factor to the system's BER, providing a higher Q-factor values correspond to lower BER values.

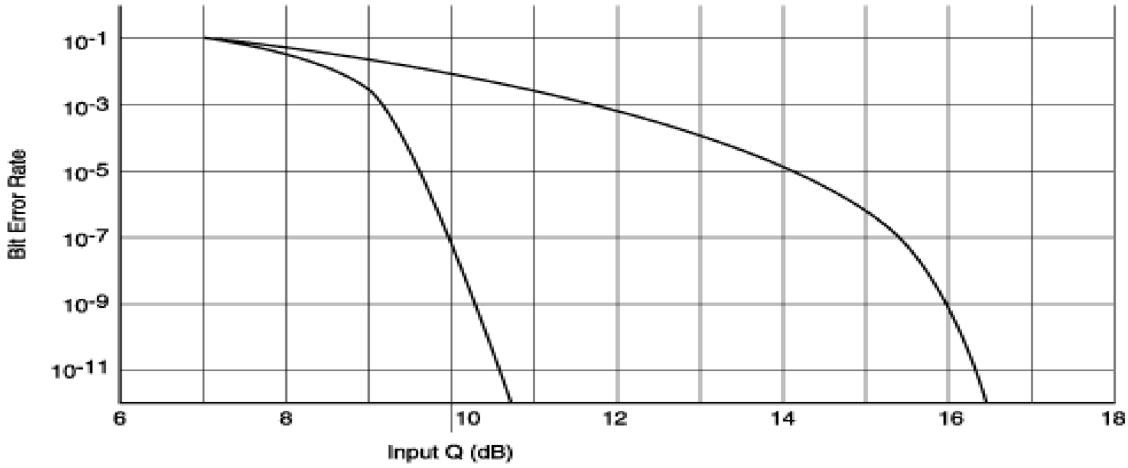

Figure I.9: *The relationship between Q to BER.*

I.5.3 Signal-to-Noise Ratio (SNR or S/N)

SNR (SNR) quantifies the ratio of received signal power to noise power, determining the achievable data rates and link reliability. In FSO systems, noise sources include shot noise, thermal noise, and amplified spontaneous emission (ASE) noise from optical amplifiers [27].

$$SNR = \frac{P_{signal}}{P_{noise}} \quad (I.5)$$

Turbulence-induced scintillation causes SNR fluctuations, necessitating adaptive techniques such as automatic gain control (AGC) or diversity reception to maintain stable performance.

I.5.4 Link Margin and Availability

The link margin represents the additional power budget beyond the minimum required for reliable operation, accounting for atmospheric attenuation (fog, rain), geometric losses, and pointing errors. System availability, often specified as a percentage of operational time (e.g., 99.9%), depends on the link margin and local weather patterns. Margins of 20–30 dB are common in terrestrial FSO systems to ensure robustness under varying conditions [16].

I.5.5 Receiver Sensitivity

The amount of optical power received at the detector is a crucial factor affecting the SNR and thus the overall performance. It is influenced by the transmitted power, atmospheric attenuation (due to absorption and scattering), geometric spread of the beam, and any misalignment losses [28].

I.5.6 Beam Divergence

An appropriate beam divergence angle is needed to optimize link performance because beam divergence can cause the received FSO signal to be larger than the aperture of the FSO receiver [27].

I.6 Conclusion

In this chapter, we have established a comprehensive understanding of Free Space Optics (FSO) communication by examining its fundamental principles, system architecture, and comparative advantages over conventional guided and unguided links. Beginning with the historical evolution from Bell's 1880 Photophone to modern laser-based systems, we highlighted how advances in optical sources, detectors, and modulation techniques have transformed FSO into a viable high-bandwidth, low-latency solution for terrestrial and space applications.

We then detailed the core components transmitter, free-space channel, and receiver emphasizing the critical influence of atmospheric effects such as fog, turbulence, and aerosols on link performance.

Key performance metrics, including bit error rate (BER), Q-factor, and signal-to-noise ratio (SNR), were introduced to quantify system reliability and guide design trade-offs. Finally, we identified the specific challenges posed by the unique climatic conditions of El-Oued, Algeria, and outlined the objectives of this thesis: to model those environmental impairments in OptiSystem, simulate a 16-QAM FSO link, and evaluate its performance under real-world weather scenarios. With this foundation, Chapter 2 will review the theoretical models of atmospheric attenuation and turbulence, paving the way for the detailed simulation and result analysis in Chapter 3.

Chapter II:

FSO System Design and Atmospheric Challenges

II.1 Introduction

Free Space Optical (FSO) communication systems exploit the properties of light to transmit high-bandwidth data through the atmosphere without the need for physical fiber. To design and optimize these systems, it is essential to understand how optical waves propagate in free space, how environmental factors modify them, and which techniques can mitigate adverse effects. This chapter lays the foundation for that understanding by exploring the fundamental physics of optical propagation, from the characteristics of the electromagnetic spectrum to the practical challenges posed by diffraction, interference, and atmospheric disturbances.

We begin with an overview of the electromagnetic spectrum and the specific wavelength windows such as near- and short-wave infrared commonly used in FSO links. Next, we introduce the basic principles of light propagation, including Huygens–Fresnel theory, Gaussian beam optics, and the origin of beam divergence. Building on these concepts, the chapter examines how coherent and incoherent sources interact, and how interference and coherence govern signal quality.

The latter sections delve into the interaction between optical beams and the atmosphere. We discuss geometric (diffraction) losses and pointing errors, and present statistical models for atmospheric turbulence, such as log-normal and Gamma distributions. The effects of weather phenomena fog, rain, and snow are analyzed through empirical attenuation models, and mitigation strategies like wavelength selection, spatial diversity, and adaptive protocols are introduced. By the end of this chapter, readers will have a clear understanding of the physical mechanisms that influence FSO performance and the tools used to predict and manage link reliability under real-world conditions.

II.2 Principles of Optical Propagation in Free Space

II.2.1 Electromagnetic spectrum and optical frequencies used in FSO

II.2.1.a Overview of the electromagnetic spectrum

The electromagnetic spectrum encompasses the full range of frequencies of electromagnetic radiation. This spectrum stretches from extremely low frequencies, such as those used in modern radio communications, to high-frequency gamma radiation, covering wavelengths that range from thousands of kilometers down to fractions of an atom's size. The limit for long wavelengths is tied to the size of the universe, while the short-wavelength limit approaches the Planck length. Various segments of this spectrum are extensively utilized in scientific research, especially for spectroscopy, as well as in communication technologies and manufacturing processes. [7][14]

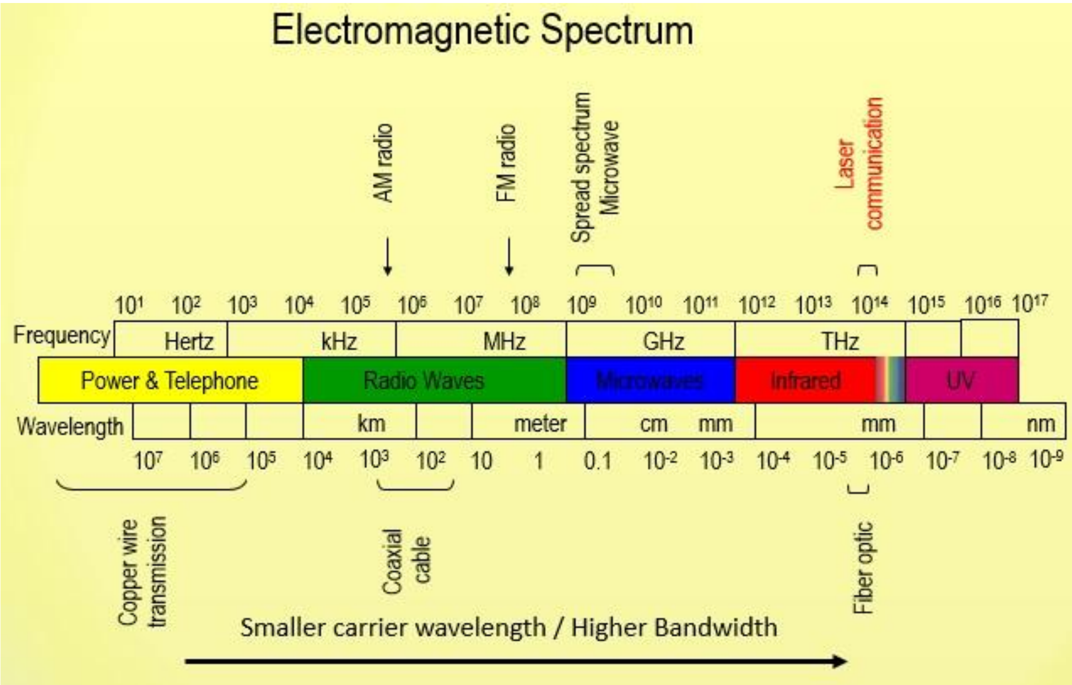

Figure II.1: *The electromagnetic spectrum. [7]*

The electromagnetic spectrum as demonstrated in *Figure II.1*, can be expressed in terms of wavelength (λ), frequency (ν), or energy. They are related by the expression, when the higher the frequency, the higher the energy.

$$\lambda = \frac{c}{\nu} \tag{II.1}$$

The energy of the various components of the electromagnetic spectrum is given by the expression:

$$E = h\nu \tag{II.2}$$

Where h is Planck's constant = 6.63×10^{-34} Joule-seconds. The units of wavelength are meters with the term's microns (denoted μm and equal to 10^{-6} m) and nanometers (10^{-9} m) being used just as frequently. Frequency is measured in (Hz), with one Hertz being equal to one cycle of one cycle of sinusoidal wave per second. A commonly used unit of energy is the electron-volt.

Wavelength selection in an FSO communication system is an important parameter as it affects the link performance and detector sensitivity of the system. The choice of wavelength strongly depends on atmospheric effects, attenuation, and background noise power. Further, the availability of transmitter and receiver components, eye safety regulations, and cost deeply impact the selection of wavelength in the FSO design process.

The International Commission on Illumination has classified optical radiations into three categories: **IR-A** (700–1400 nm), **IR-B** (1400–3000 nm), and **IR-C** (3000 nm–1 mm). It can be subclassified into:

- **Near-infrared (NIR)** ranging from 750 to 1450 nm which is a low attenuation window and used for optical fiber.
- **Short-infrared (SIR)** ranging from 1400 to 3000 nm out of which 1530-1560 nm is a dominant spectral range for long-distance communication.

All commercially available FSO systems use NIR and SIR wavelength range since these wavelengths are also used in optical fiber communication, and their components are readily available in the market. [13]

Common FSO wavelengths used are:

➢ The 850 nm window is characterized by low attenuation, making it highly suitable for free space optics (FSO) operation. This wavelength range benefits from the availability of reliable, high-performance, and cost-effective transmitter and detector components that are widely used in modern service provider networks and transmission equipment. Extremely sensitive Silicon avalanche photodiode (APD) detector technology can be used alongside advanced laser technology.

➢ The 1550 nm band is ideal for free space transmission, primarily due to its low attenuation and the abundance of high-quality transmitter. This includes very high-speed semiconductor laser technology that is conducive to wavelength division multiplexing (WDM) operations, as well as amplifiers such as erbium-doped fiber amplifiers (EDFA) and semiconducting optical amplifiers (SOA) that help boost transmission power. Thanks to these favorable attenuation properties and the availability of advanced components, the development of WDM free space optical systems is both practical and achievable. [7]

II.2.1.b Advantages of optical frequencies

1. **High Security:** The use of directional and narrow beam width lasers enhances security for transmitting sensitive information, such as legal, financial, and military data.

2. **Increased Channel Capacity:** Optical frequencies provide a vast modulation bandwidth, allowing for high data rates, which is essential for modern communication needs.

3. **Electromagnetic Immunity:** Photonic signals do not produce electromagnetic interference (EMI) and cannot be detected using RF meters or spectrum analyzers, ensuring electric isolation and enhanced security.

4. **Environmentally Friendly:** Optical systems utilize invisible, eye-safe laser beams, making them a clean and sustainable technology that poses minimal risk to the environment.

5. **License-Free Operation:** Optical communication systems do not require frequency allocation or spectrum regulation, simplifying deployment and reducing costs.

6. **Reduced Multipath Propagation:** The highly focused nature of optical beams minimizes multipath effects, which can lead to reduced signal fading and improved communication reliability.

7. **Excellent Power Efficiency: With low power consumption and a short beam** divergence angle, optical systems ensure efficient energy use, further enhancing their viability.

8. **Compact and Lightweight Equipment:** Optical communication systems are designed to be minimal in size and weight, facilitating ease of deployment and installation in varied environments. These advantages make optical frequencies a compelling choice for various applications in telecommunications and data transmission. [29]

II.2.2 Basic Concepts of Light Propagation

II.2.2.a Diffraction

a. The Huygens-Fresnel principle

According to Huygens' construction, every point of a wavefront can be treated as a center of a secondary disturbance, which leads to the generation of spherical wavelets. At any future moment, the wavefront can be considered the envelope of these wavelets. Fresnel expanded on this idea by proposing that these secondary wavelets interfere with one another, resulting in what is known as the *Huygens–Fresnel principle*. Before applying this principle to explore diffraction effects, it is essential to confirm that it accurately describes the propagation of light in free space, with a few simple additional assumptions.

Let (*Figure II.2)* denote the instantaneous position of a spherical monochromatic wavefront of radius r_0 originating from a point source P_0 . We aim to assess the light disturbance at a particular point P. Omitting the time periodic factor $e^{-i\omega t}$, the disturbance at a point Q on the wavefront can be characterized by the expression: Ae^{ikr_0}/r_0 where A indicates the amplitude at unit distance from the source. Following the Huygens–Fresnel principle, each element of the wavefront is regarded as the center of a secondary disturbance that propagates as spherical wavelets. Therefore, the contribution $dU(P)$ from the element dS at point Q can be expressed as follows:

$$dU(P) = K(\chi)\frac{Ae^{ikr_0}}{r_0}\frac{e^{iKs}}{s}dS \tag{II.3}$$

Where $s = QP$ and $K(\chi)$ is an *inclination factor* which describes the variation with direction of the amplitude of the secondary waves, χ being the angle (often called the *angle of diffraction*) between the normal at Q and the direction QP.

This expression represents how the disturbance at point P can be determined by summing the contributions from all elements of the wave-front, adhering to the principle of superposition inherent in the Huygens–Fresnel approach. [30]

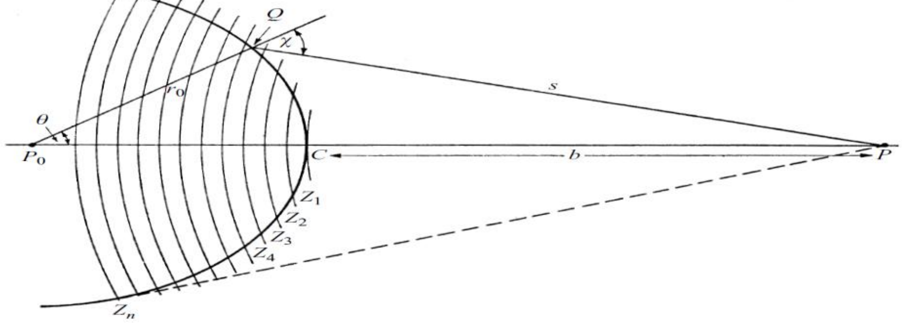

Figure II.2: *Fresnel's zone construction. [30]*

b. Diffraction-limited beam divergence

➢ **Beam Divergence Loss:** As the optical beam propagates through the atmosphere, it spreads out due to diffraction. This may result in a situation where the receiver aperture is not able to collect a fraction of the transmitted beam, leading to beam divergence loss as depicted in *Figure II.3* A typical free-space optical system transmits an optical beam with a certain aperture diameter D_T. Due to diffraction, this beam expands as it travels, increasing in diameter over a distance. The receiver, with a limited aperture diameter D_R, may only capture a portion of the transmitted beam, leading to power loss [13]. The optical power collected by the receiver is given by the following:

$$P_R = P_T G_T G_R L_P \tag{II.4}$$

P_T is the transmitted power, L_P is the free-space path loss, and G_T and G_R are the effective antenna gains of the transmitter and receiver, respectively. [13]

Substituting the values:

$$L_P = \frac{\lambda}{4\pi R}^2 \quad , \quad G_T \approx \frac{\pi D_T{}^2}{\lambda} \quad , \quad G_R \approx \frac{\pi D_R{}^2}{\lambda}$$

The received optical power is obtained as:

$$P_R \approx P_T \frac{D_T D_R}{\lambda R}^2$$

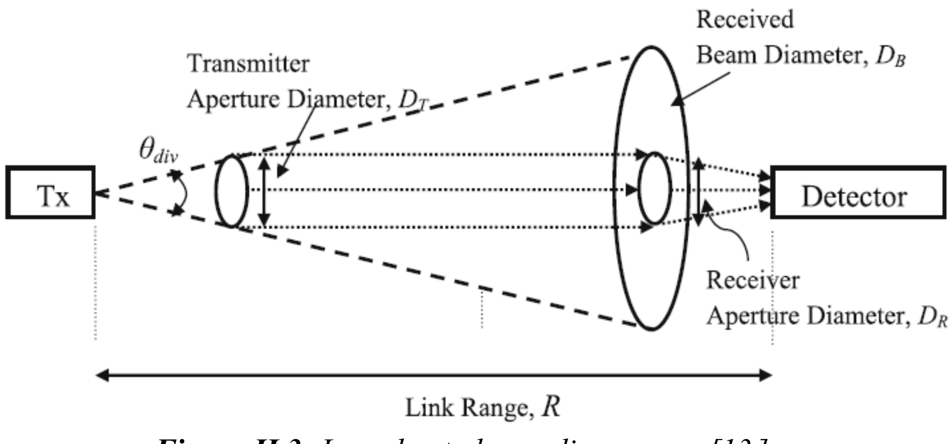

Figure II.3: *Loss due to beam divergence. [13]*

➢ **Diffraction-Limited Beam Divergence Loss**: The diffraction-limited beam divergence loss, sometimes referred to as geometric loss, can be expressed in decibels:

$$L_G = -10\ 2log\frac{4}{\pi} + log\frac{A_T A_R}{\lambda^2 R^2} \tag{II.5}$$

An optical source with a narrow beam divergence is preferable because it minimizes power loss. However, if the beam is excessively narrowed, it increases the system's sensitivity to misalignment between transceivers. Thus, it's essential to choose a beam divergence that balances control with system stability. [13]

The diffraction-limited divergence angle is given by:

$$\theta_{div} \approx \frac{\lambda}{D_T} \tag{II.6}$$

An increased transmitter aperture (D_T) diminishes diffraction, yielding a more collimated beam with less dispersion. On the other hand, a reduced aperture amplifies diffraction, which can markedly increase beam divergence and decrease the amount of transmitted power that the receiver can catch.

In a non-diffraction-limited case, where the source has an initial divergence angle θ_{div}, the beam size at a certain distance R is given by $\boldsymbol{D_T} + \theta_{div}R$, leading to the power fraction received:

$$\frac{P_R}{P_T} = \frac{D_R^2}{(D_T+\theta_{div}R)^2} \tag{II.7}$$

The corresponding beam divergence loss in decibels is:

$$L_G = -20\, log\, \frac{D_R}{D_T+\theta_{div}R} \tag{II.8}$$

- **Beam Expanders for Divergence Control:** to counteract diffraction-induced divergence, beam expanders may be utilized. A beam expander increases the initial beam diameter prior to transmission, reducing divergence θ_{div} and enhancing optical power reception over longer distances, as shown in *Figure II.4.*

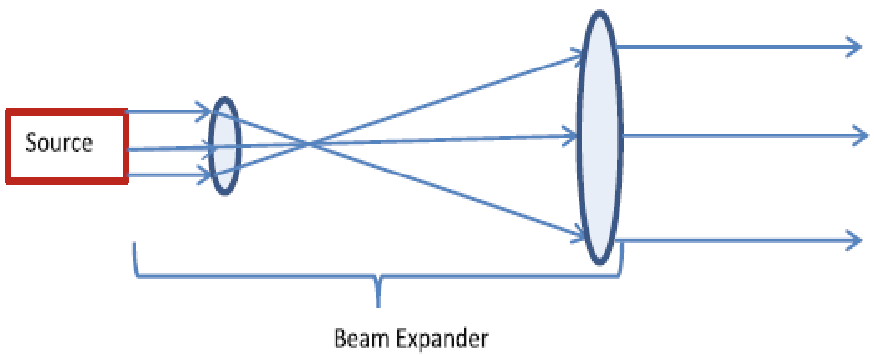

Figure II.4: *Beam expander to increase diffraction aperture. [13]*

II.2.2.b Interference in wave phenomena

1. **Coherent sources** generate waves with a constant phase relationship, ensuring crests and troughs align over time. These waves are "in phase" and exhibit a consistent phase difference, fixed frequency and wavelength, monochromatic singular frequency, and spatial and temporal correlation, ensuring a consistent link across both dimensions.
2. **Incoherent sources** emit waves with random and unpredictable phase relationships. The peaks and troughs from these sources do not maintain consistent alignment, resulting in waves that are out of phase. These waves typically contain multiple frequencies and varying amplitudes, making them non-monochromatic. Common examples include sunlight and conventional light bulbs, which lack the spatial and temporal coherence needed for precise wave interference experiments.
3. **Constructive interference** occurs when identical frequencies and phase pairs combine, producing increased amplitude waves. This results in bright bands in light interference patterns, amplified sound in acoustics, and enhanced signal strength in communication systems.
4. **Destructive interference** occurs when opposite phases of waves interact, leading to partial or complete cancellation of wave amplitudes. This creates dark fringes in optical interference, enables noise-canceling technologies, and can cause signal degradation in wireless communications. [31]

II.2.2.c Coherence

Coherence is a fundamental concept in optics that refers to the consistent phase relationship between electric field values across various locations or times. Partial coherence refers to scenarios with a degree of correlation between phase values, although it's not perfect. Coherent and incoherent terms are used to describe processes or techniques, with "coherent" indicating phase-sensitiveness. Coherent beam combining relies on mutual coherence of incoming beams, while spectral (incoherent) beam combining operates without phase dependency. [32]

- **Spatial Coherence (Beam Uniformity)** produces beams with exceptional spatial coherence, characterized by uniform wavefronts and intensity profiles. This is due to the resonant cavity's ability to enforce phase relationships, creating spatially correlated electromagnetic field patterns. This contrasts with conventional light sources, enabling precise beam control in applications like holography, optical trapping, and interferometric measurements.

➢ **Temporal Coherence (Linewidth)** in lasers is determined by their spectral purity and linewidth. Single-frequency lasers achieve sub-hertz linewidths, serving as optical frequency standards for metrology and atomic clocks. However, multiple longitudinal modes can broaden linewidth and reduce coherence. Even single-frequency lasers can suffer from phase noise, which can be mitigated by active stabilization techniques like optical feedback or atomic references.

II.2.3 Gaussian Beam Propagation

II.2.3.a Fundamental Gaussian beam characteristics

1. **Beam Waist (w_0)**

The beam waist (w_0) refers to the point along the beam's axis where its radius is smallest. It represents the narrowest section of the beam and is typically found at the focal point of an optical system. The size of the beam waist influences its divergence and focusing properties, making it a key factor in optical communication and laser-based applications.

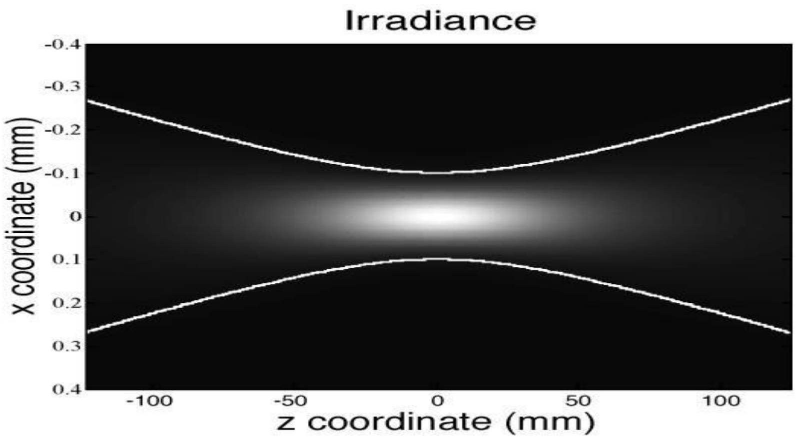

Figure II.5: *Irradiance distribution of a Gaussian beam. The bright spot is beaming waist. [29]*

The beam waist size of a Gaussian beam is given by:

$$w(z) = w_0 \sqrt{1 + \frac{z}{z_R}^2} \tag{II.9}$$

Where:

- $\boldsymbol{w(z)}$ is the beam radius at a given distance.
- $\boldsymbol{w_0}$ is the beam waist radius (at the narrowest point).
- $\boldsymbol{z_R}$ is the Rayleigh range.

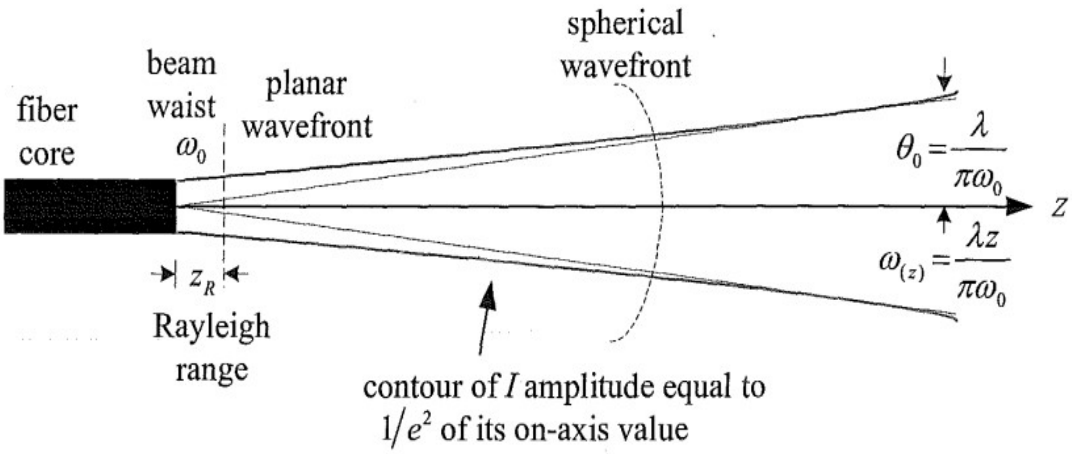

Figure II.6: *Gaussian beam propagating from a fiber core to free space. [29]*

2. **Divergence Angle (θ)**

The beam's angular divergence is expressed as:

$$\theta = \frac{\lambda}{\pi w_0} \tag{II.10}$$

This equation highlights the inverse relationship between divergence and waist width. While θ is not an accurate representation near the beam waist, it becomes more precise at greater distances. A smaller beam waist leads to greater divergence, whereas a larger waist helps in maintaining collimation over longer distances. [29]

3. **Rayleigh Range (z_0)**

To understand how a Gaussian beam spreads due to diffraction, the Rayleigh range is an essential parameter. It defines the distance from the beam waist to the point where the beam spot size doubles ($w = \sqrt{2}w_0$), given by:

$$z_R = \frac{\pi w_0^2}{\lambda} \tag{II.11}$$

at $z = z_R$, the radius of curvature is at its minimum, indicating maximum beam focus. As the beam expands, the axial size of the waist increases quadratically, improving the region of collimation. [29]

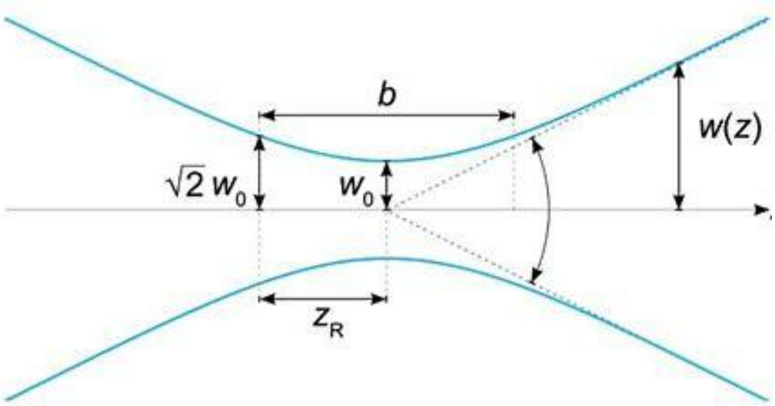

Figure II.7: *Rayleigh range and confocal parameter of a Gaussian beam. [29]*

II.2.3.b Impact of Beam Divergence on Link Alignment and Pointing Losses

1. Causes of Beam Divergence

Three primary atmospheric effects impact optical wave propagation in free space: scattering, absorption, and optical turbulence. Scattering occurs when atmospheric particles such as dust and aerosols interact with the beam, redirecting its energy. Absorption leads to energy loss as the beam interacts with gas molecules in the atmosphere. Optical turbulence, caused by temperature-induced variations in the refractive index, distorts the beam, resulting in intensity fluctuations, beam broadening, beam wander, and even beam breakup.

While scattering and absorption primarily contribute to laser beam attenuation, optical turbulence degrades beam quality by causing dynamic distortions and spatial instability. The Beam Quality Factor is given as [29]:

$$M^2 = \frac{\pi w_0 \theta}{\lambda} \tag{II.12}$$

Where M^2 indicates how closely the beam resembles an ideal Gaussian beam.

2. Beam Wander and Misalignment Issues

Beam wander arises due to fluctuations in the refractive index, causing random displacements of the beam's centroid. This leads to pointing errors and power loss at the receiver. Additional factors such as mechanical instability, environmental vibrations, and slight misalignments further decrease received power and overall system performance. [29]

The pointing error model can be presented with the formula:

$$P_e = e^{-(\frac{\Delta\theta}{\theta})^2} \tag{II.13}$$

- $\boldsymbol{P_e}$ is the probability of a pointing error
- $\boldsymbol{\Delta\theta}$ represents the misalignment angle
- $\boldsymbol{\theta}$ is the beam divergence angle

II.3 Atmospheric Effects on Optical Signals

II.3.1 Atmospheric Attenuation

Atmospheric attenuation significantly impacts the performance of Free Space Optical (FSO) communication systems. It refers to the reduction in the intensity of an optical beam as it propagates through the atmosphere. This reduction is caused by several factors: absorption by atmospheric gases, scattering by aerosols, and molecular scattering [33].

II.3.2 Factors contributing to Atmospheric Attenuation

II.3.2.a Absorption by Atmospheric Gases

Certain gases in the atmosphere, such as water vapor (H_2O), carbon dioxide (CO_2), and ozone (O_3), absorb photons from the optical beam, converting light energy into heat [17]. This absorption reduces the signal strength [16].

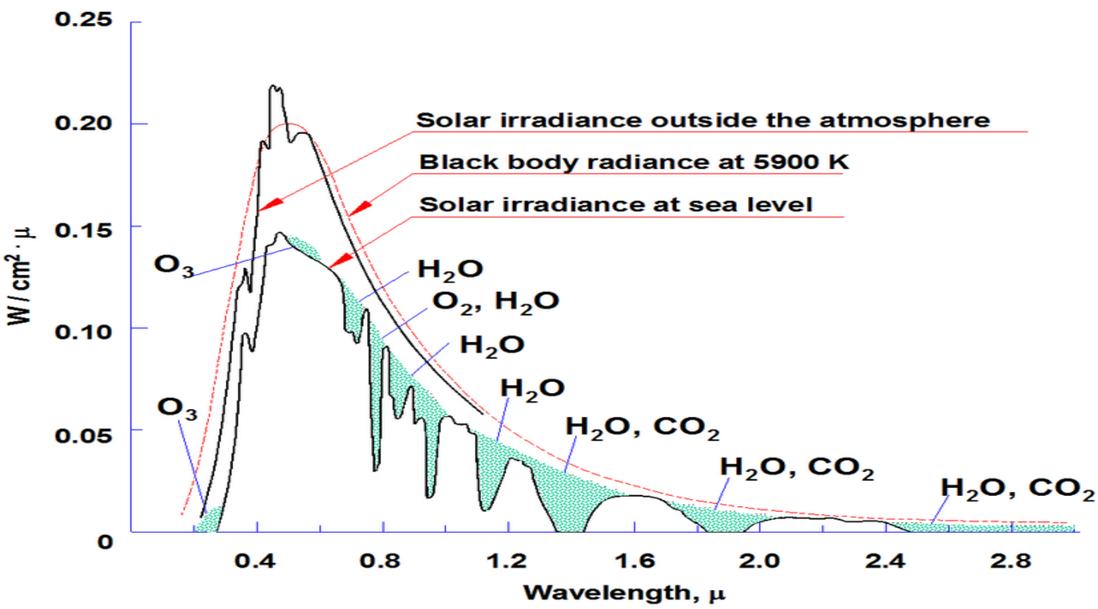

Figure II.8: *Solar Spectra and absorption bands of atmospheric gases. [34]*

II.3.2.b Scattering by Aerosols

Aerosols, which include dust, fog, haze, smoke, and other particulate matter, scatter the optical signal. The size of these particles is comparable to the wavelength of the light, leading to significant attenuation [35][33].

Type	Radius(μm)	Size parameter	Scattering parameter
Air molecules	0.0001	0.00074	Rayleigh
Fog droplet	1-20	7.4-147.8	Mie- Geometrical
Rain	100-10000	740-74000	Geometrical
snow	1000-5000	7400-37000	Geometrical

Table II.1: *Typical atmospheric scattering particles with their radii and scattering process at λ =850nm.*

II.3.2.c Molecular (Rayleigh) Scattering

This type of scattering occurs when light interacts with air molecules. It is more prominent at shorter wavelengths, especially below 1μm (ultraviolet or visible range) [16].

II.3.3 Impact of Atmospheric Conditions on FSO system

a. **Weather Conditions:** Heavy rain, fog, snow, and dust introduce severe attenuation, reducing link reliability. Among these, fog is particularly detrimental due to its high particle density, causing substantial signal attenuation [36][29].

b. **Visibility:** Low visibility conditions, often caused by high concentrations of airborne particles (e.g., haze or smog), increase scattering losses, further weakening the transmitted optical signal.

c. **Optical Turbulence:** atmospheric turbulence, driven by temperature and pressure variations, induces refractive index fluctuations. This leads to scintillation (signal irradiance fading), beam wandering, and spatial distortion, reducing channel capacity and limiting transmission distance [16][29].

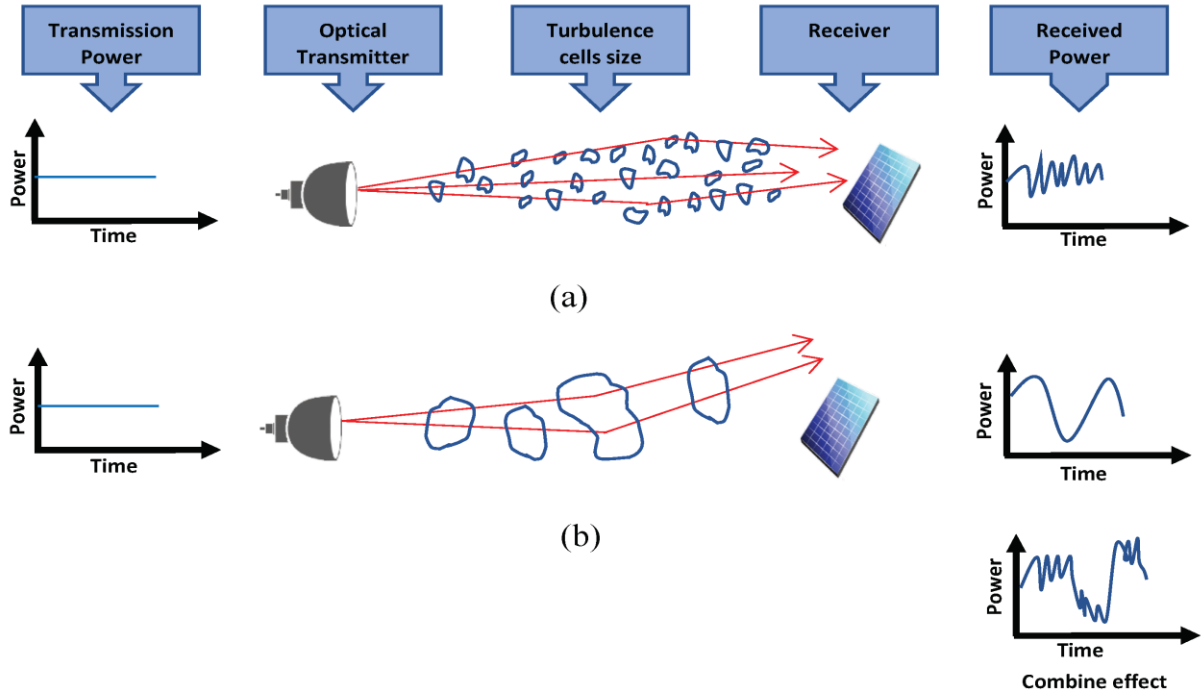

Figure II.9: *Comparison of Turbulent Cell Size with (a) Scintillation and (b) Beam Wander. [37]*

II.3.4 Mitigation Techniques for Atmospheric Effects

To combat the challenges posed by atmospheric conditions in Free-Space Optical (FSO) communication, several mitigation strategies have been developed:

- **a. Wavelength Selection:** Choosing an optimal transmission wavelength (near infrared or short-wave infrared bands) helps minimize absorption and scattering losses. Proper wavelength selection is critical for maximizing link performance in different weather conditions [16].
- **b. Polarization Diversity**: Transmitting redundant data streams using orthogonal polarizations can mitigate turbulence-induced signal degradation. This technique improves reliability by exploiting the polarization stability of optical signals.
- **c. Spatial Diversity**: Deploying multiple transmitter beams or receiver apertures reduces the impact of turbulence-induced fading. By leveraging independent fading paths, spatial diversity enhances signal robustness and link availability [35].
- **d. Adaptive Protocols**: Dynamic congestion control and rate-adaptive transmission protocols optimize FSO network throughput under varying atmospheric conditions. These protocols adjust transmission parameters in real-time to maintain efficient data delivery [16].

II.3.5 Beer-Lambert Law

The transmittance of an optical signal propagating through the atmosphere is described by the Beer-Lambert law [38]:

$$\tau = exp(-\beta L) \quad \text{(II.14)}$$

Where τ is the transmittance, β is the total attenuation coefficient, and L is the distance the light travels.

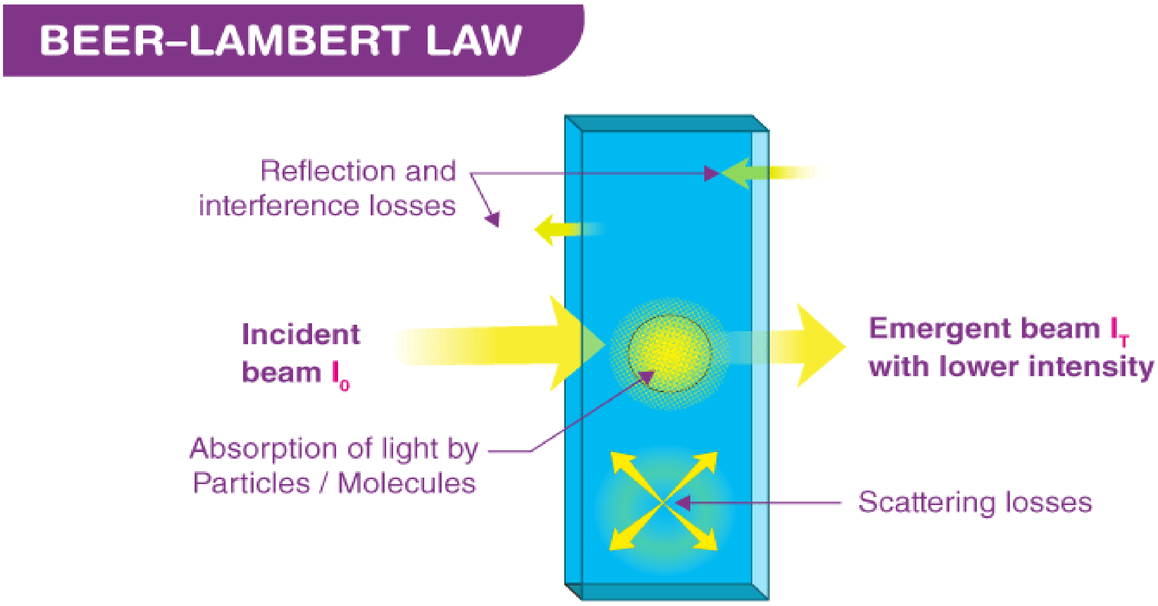

Figure II.10: *Schematic Diagram of Beer-Lambert Law. [38]*

Total attenuation is often expressed as a combination of the absorption coefficient and the scattering coefficient, especially in optical systems like biology or atmospheric sciences.
In such cases, the total attenuation α is given by:

$$I = I_0 e^{-\alpha l} \quad \text{(II.15)}$$

Where:

- I is the transmitted light intensity,
- I_0 is the initial light intensity,
- α is the total attenuation coefficient (cm^{-1}), which is the sum of the absorption and scattering coefficients,
- l is the path length.

The total attenuation coefficient α can be expressed as:

$$\alpha = \alpha_{abs} + \alpha_{sca} \quad \text{(II.16)}$$

Where:

- α_{abs} is the absorption coefficient,
- α_{sca} is the scattering coefficient.

Thus, the Beer-Lambert law is focused on absorption, while total attenuation accounts for both absorption and scattering of light.

II.4 Atmospheric Turbulence

Reliable applications of free space optical communication technologies are significantly hampered by atmospheric turbulence. Driven mostly by variations in temperature and pressure, this phenomenon results from random changes in the optical qualities of the environment. Most importantly refractive index fluctuations, scintillation, and beam spreading, these variations cause several negative impacts on the propagating optical signal. Designing strong FSO linkages [39] depends on an awareness of these impacts and the statistical models applied to describe them.

II.4.1 Refractive index fluctuations

Atmospheric turbulence originates from the inhomogeneities in air temperature and pressure, as well as wind velocity variations, which create turbulent eddies of varying densities [16] [39] [27].

These eddies cause rapid and random fluctuations in the refractive index of the air along the optical propagation path. The refractive index, a measure of how much the speed of light is reduced in a medium, becomes spatially and temporally variable. These refractive index fluctuations act like a series of constantly changing lenses or prisms, causing the optical beam to be randomly refracted and diffracted as it travels through the atmosphere [40].

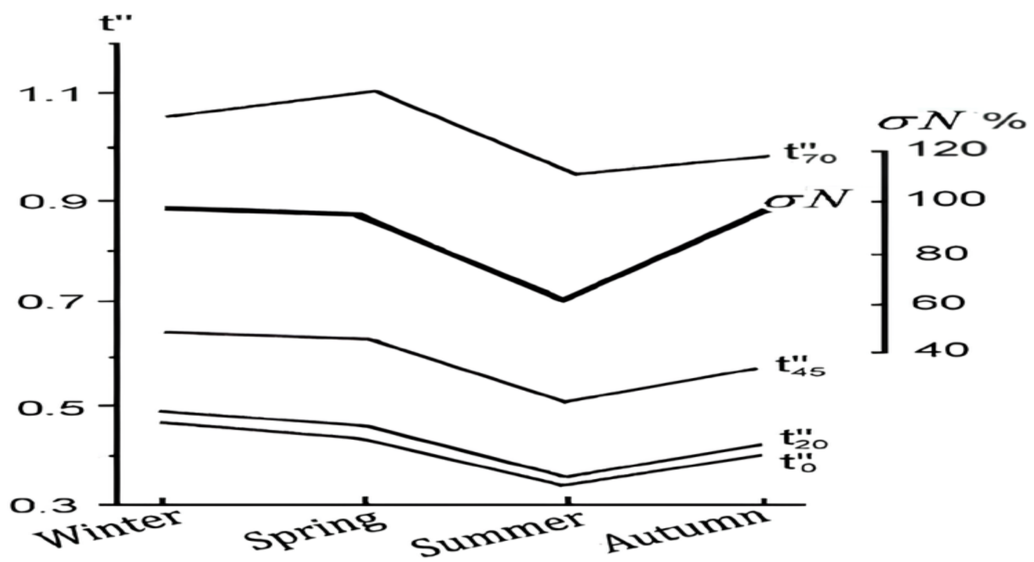

Figure II.11: *Scheme showing the Seasonal changes of refractive index fluctuations. [40]*

The relationship between the refractive index and atmospheric conditions can be complex. However, this equation provides a simplified relation to the rate of change in the index of refraction with temperature:

$$n = 1 + 77.6\ x\ 10^{-6} \frac{P}{T}\left(1 + \frac{7.52\ x\ 10^{-3}}{\lambda^2}\right) \quad \text{(II.17)}$$

Where P is the pressure in Pascals and T is the temperature in Kelvin. This equation highlights the dependence of the refractive index on temperature and pressure [38]. The refractive index structure parameter, C_n^2 , is a fundamental value used to measure atmospheric turbulence degree and the strength of these refractive index variations. Usually, it is stated as a fundamental determinant of the variation in the atmospheric refractive index, evaluating the consequences of air turbulence [41] [42].

II.4.2 Scintillation Effects

The random refractive index variations along the propagation path led to two primary effects on the optical signal: scintillation and beam spreading.

Scintillation, also known as intensity fluctuations or irradiance fluctuations, refers to the rapid and random variations in the intensity of the received optical signal [16][32][44]. This phenomenon is analogous to the twinkling of stars. As the coherent laser beam propagates through the turbulent atmosphere, it encounters air pockets with varying refractive indices, causing scattering and interference. This interference, both constructive and destructive, results in temporal and spatial fluctuations of the light intensity at the receiver [16][41]. Scintillation is more pronounced over longer transmission distances and can significantly degrade the bit error rate (BER) of the FSO link.

The severity of scintillation is influenced by factors like temperature gradients, wind speeds, and the propagation distance [45]. A quantitative measure of scintillation is the scintillation index σ_I^2, which is the normalized variance of the irradiance, defined as:

$$\sigma_I^2 = \frac{\langle I^2 \rangle}{\langle I \rangle^2} - 1 \quad \text{(II.18)}$$

Where I is the received optical intensity and $\langle\cdot\rangle$ denotes the ensemble average.

II.4.3 Beam spreading

It is another consequence of atmospheric turbulence. As the laser beam propagates through the turbulent medium, the random refractive index gradients cause the beam to spread out more than it would in free space. This increased beam size at the receiver reduces the optical power density, leading to a weaker received signal. The extent of beam spreading is influenced by the turbulence strength and the propagation distance [11][31].

Larger turbulence eddies (with dimensions bigger than the beam radius) can also cause beam wander, where the entire beam deviates randomly from its intended path [45]. Thus, the time-averaged irradiance of the beam can be expressed as:

$$I(l,r) = \frac{2P_0}{\pi\omega_{eff}^2(1)} exp\left(\frac{-2r^2}{w_{eff}^2(1)}\right) \quad \text{(II.19)}$$

Where: P_o is total beam power in W and r is the radial distance from the beam center.
The beam will undergo a deterioration in quality, resulting in an average beam waist over time of $\omega_{\text{eff}}(l) > \omega(l)$ [11].

To quantify the extent of beam spreading, the effective beam waist average is defined as:

$$\omega_{\text{eff}}(l)^2 = \omega(l)^2(1+T) \quad \text{(II.20)}$$

Where $\omega(l)$ is the beam waist that after propagation distance L is given by:

$$\omega(l)^2 = [\omega_0^2 + (\frac{2L}{k\omega_0})^2](m^2) \quad \text{(II.21)}$$

Where ω_0 denotes the initial beam waist at $L = 0$, and T represents the additional beam spreading induced by turbulence. Like other turbulence-related figures of merit, T is influenced by the turbulence strength and the beam propagation path. Specifically, for a horizontal propagation path, T is given by:

$$T = 1.33\, \sigma_i^2\, \Lambda^{\frac{5}{6}} \quad \text{(II.22)}$$

While the parameter Λ is given by:

$$\Lambda = \frac{2L}{k\omega^2(l)} \quad \text{(II.23)}$$

The effective beam waist, denoted as $\omega_{\text{eff}}(l)$, characterizes the long-term averaged variation in beam irradiance.

As observed in other turbulence-related figures of merit, the squared effective waist, $\omega_{\text{eff}}(l)^2$, is influenced by both turbulence intensity and the propagation path of the beam. Notably, since $\omega_{\text{eff}}(l)$ exceeds $\omega(l)$, the beam will experience a power loss at its center, which can be quantified as:

$$L_{BE} = 20\log_{10}(\frac{\omega(l)}{\omega_{\text{eff}}(l)}) \quad \text{(II.24)}$$

II.4.4 Statistical Turbulence Models

Statistical models are utilized to characterize the impact of atmospheric turbulence on the optical signal due to its random nature. Numerous probability density functions (PDFs) have been suggested to represent the irradiance fluctuations caused by turbulence [32][39]. The predominant models utilized include the log-normal, Gamma-Gamma, and K-distribution.

II.4.4.a Log-normal Distribution

This model assumes that the logarithm of the received irradiance follows a normal (Gaussian) distribution. The log-normal model is mathematically convenient and tractable [47] and is most applicable under weak turbulence conditions, where the Irradiance fluctuations are small, and single scattering events dominate [27][39].
The lognormal distribution is given by:

$$p_I(I) = \frac{1}{I\sigma\sqrt{2\pi}} \exp\left(-\frac{(\ln I-\mu)^2}{2\sigma^2}\right) \tag{II.25}$$

Where μ is the logarithmic mean and σ^2 is the logarithmic variance

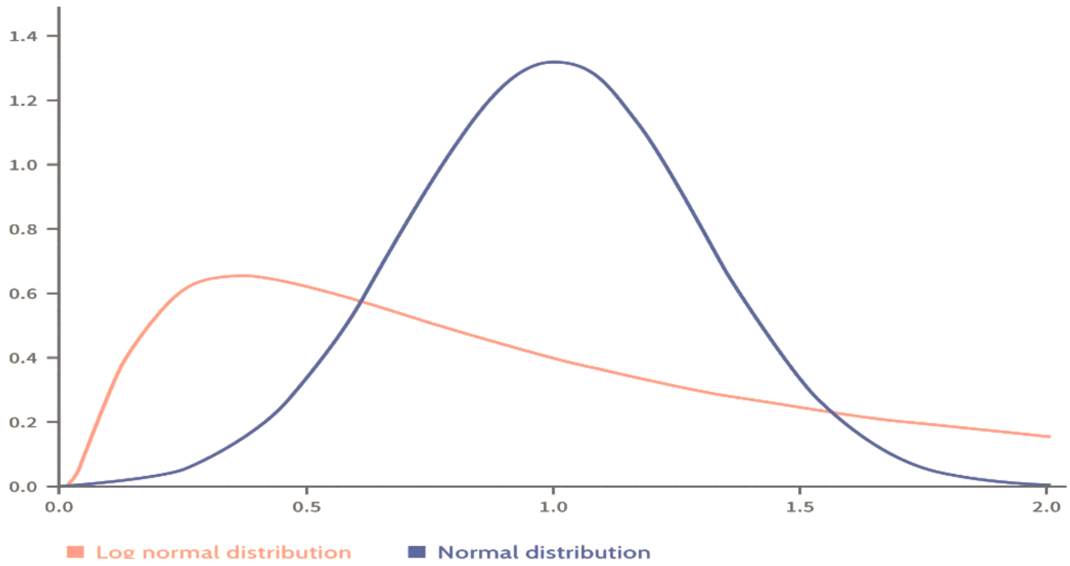

Figure II.12: *The difference between normal and log-normal Distribution. [24]*

II.4.4.b Gamma-Gamma Distribution

The Gamma-Gamma model is a versatile analysis tool that considers both small-scale (scintillation) and large-scale (beam wander) effects of turbulent atmosphere on optical signals. It accurately represents a wide range of turbulence conditions, from weak to strong, and is widely used in the analysis of FSO links [46][47]. The model's probability density function for received irradiance I is given by:

$$p(I) = \frac{2(\alpha\,\beta)^{(\alpha+\beta)/2}}{\Gamma(\alpha)\Gamma(\beta)} I^{\left(\frac{\alpha+\beta}{2}\right)-1} K_{\alpha-\beta}\sqrt{(2\,\alpha\,\beta\,I)} \quad \text{(II.26)}$$

Where:

- α and β are parameters related to the effective number of large-scale and small-scale eddies.
- $K_n(x)$ is the modified Bessel function of the second kind of order $\alpha - \beta$ and $\Gamma(x)$ is the Gamma function [27] .

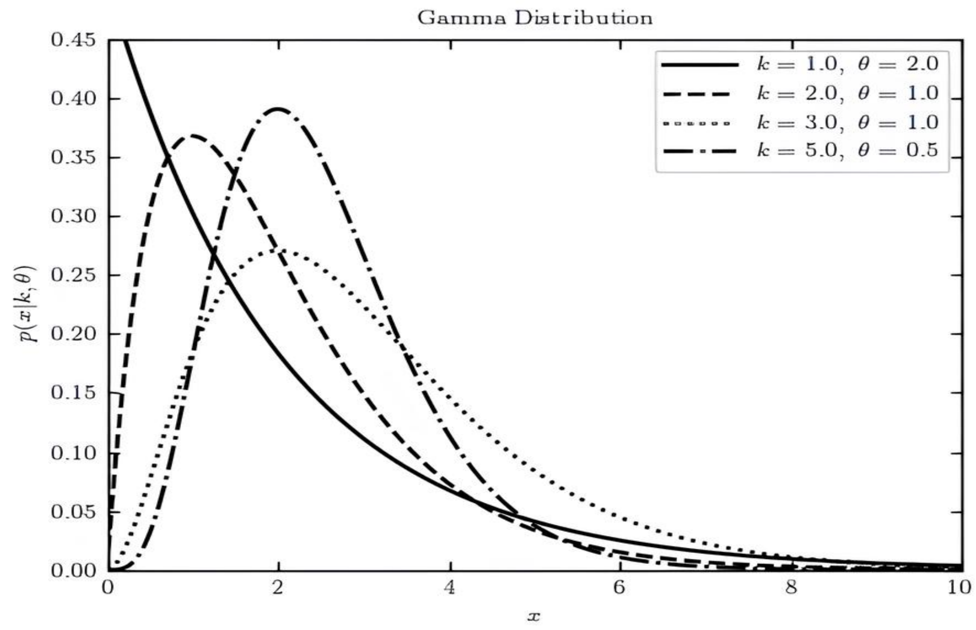

Figure II.13: *Example of a Gamma distribution.*

II.4.4.c K-Distribution

The K-distribution model is another statistical model used to characterize irradiance fluctuations, particularly under moderate to strong turbulence conditions [27]. It is often found to match experimental data better in stronger turbulence regimes compared to the log-normal model. The K-distribution arises from considering the received signal as a superposition of a random number of scattered waves [39].

The probability density is the K-distribution is given by:

$$p_I(I) = \frac{2(\mu_y)^{\mu_y}}{\Gamma(\mu_y)} I^{\mu_y-1} K_{\mu_y-1}(2\sqrt{\mu_y I}) \quad \text{(II.27)}$$

Where $K_{\mu_y-1}(x)$ is the modified Bessel function of the second kind, and $\Gamma(\mu_y)$ is the Gamma function.

II.5 Weather Effects

Free space optics communication, despite its high bandwidth and license-free operation, is highly susceptible to atmospheric conditions, particularly weather, which can cause signal attenuation and link reliability.

II.5.1 Fog

Fog, composed of suspended water droplets with sizes comparable to the wavelengths used in FSO systems (typically in the visible and near-infrared regions), poses a significant challenge due to Mie scattering [33]. This type of scattering occurs when the size of the atmospheric particles is like the wavelength of the propagating light, leading to considerable attenuation of the optical signal [16] [24].

II.5.1.a Visibility and Attenuation

The density of fog is inversely related to visibility; increased fog density leads to diminished visibility. Thus, diminished vision results in heightened attenuation of the FSO signal. In instances of thick fog (visibility under 50 meters), signal attenuation may surpass 350 dB/km. In contrast, once visibility exceeds 1 km, the attenuation caused by fog diminishes, nearing nil at extensive visibility ranges [11] [16] [29].

II.5.1.b Empirical Models for Fog Attenuation

Several empirical models have been developed to predict fog attenuation based on visibility. One commonly used model is Kim's experimental model for Mie scattering, given by:

$$\beta_{\text{fog}} = \frac{3.91}{V}\left(\frac{\lambda}{\lambda_0}\right)^{-p} \tag{II.28}$$

Where V (in km) represents the visibility distance, λ (in nm) denotes the operating wavelength, λ_0 is the reference wavelength, and p is the scattering size distribution coefficient.
This equation is commonly used to estimate signal attenuation due to fog in optical and wireless communication systems.

Another set of models are the Kruse models, also relating attenuation to visibility [30]. These models highlight the strong dependence of FSO link performance on fog density and the associated reduction in visibility.

Figure II.14 visually demonstrates the inverse relationship between attenuation and visibility distance in foggy conditions observed in Abidjan. *Figure II.15* further illustrates the monthly variation of fog-induced attenuation in the same region, showing low maximum attenuation due to fog compared to rain in that specific climate.

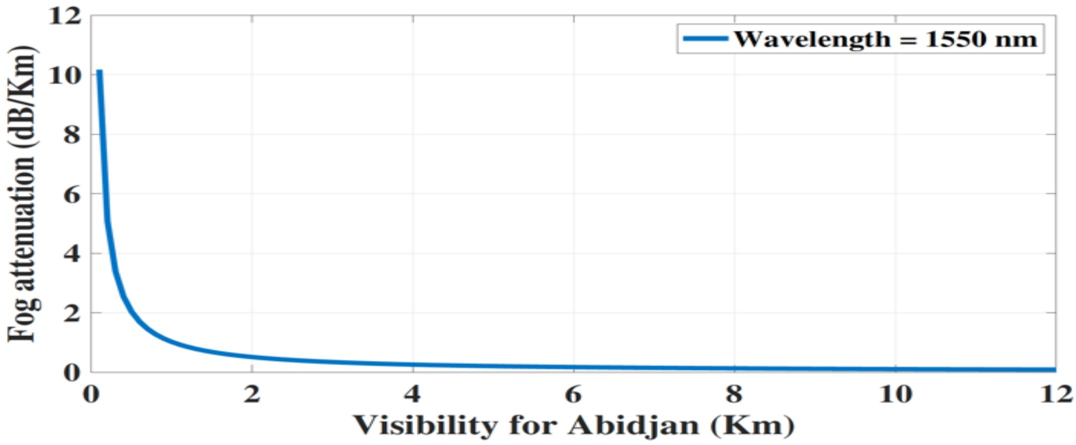

Figure II.14: *Attenuation due to fog as a function of visibility distance in Abidjan. [39]*

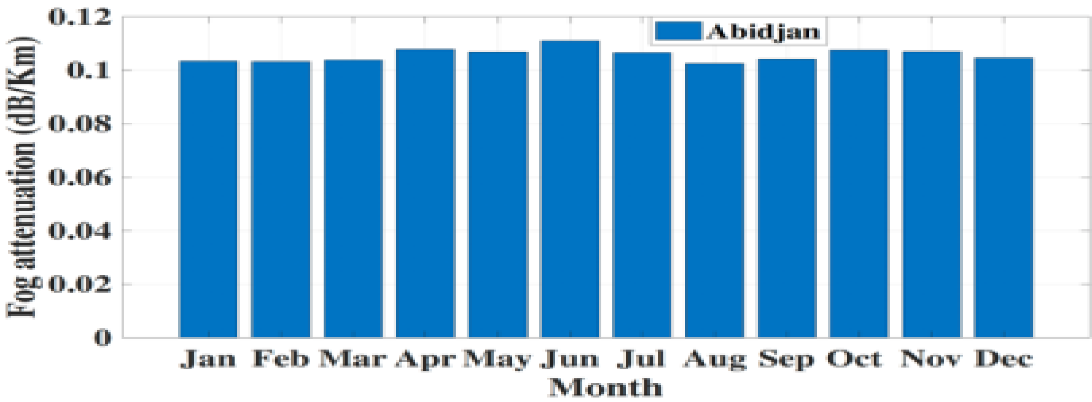

Figure II.15: *Attenuation due to fog as a function of visibility distance in Abidjan. [39]*

II.5.2 Rain

Rain, characterized by water droplets significantly larger than the wavelengths used in FSO system, primarily causes attenuation through scattering and absorption. The larger size of raindrops leads to non-selective scattering, where the attenuation is less dependent on the wavelength in the optical range compared to fog [39].

II.5.2.a Rain Rate and Attenuation

The degree of attenuation due to rain is highly dependent on the rainfall rate (R), typically measured in mm/hr [39] [28]. Higher rain rates result in greater signal attenuation. For instance, heavy rain (25 mm/hr) can cause significantly higher attenuation (around 10 dB/km at 1500 nm) compared to light rain (2.5 mm/hr, around 1 dB/km at 1500 nm) [16]. In tropical regions like Malaysia, attenuation due to heavy rain can be as high as 60 dB/km [33].

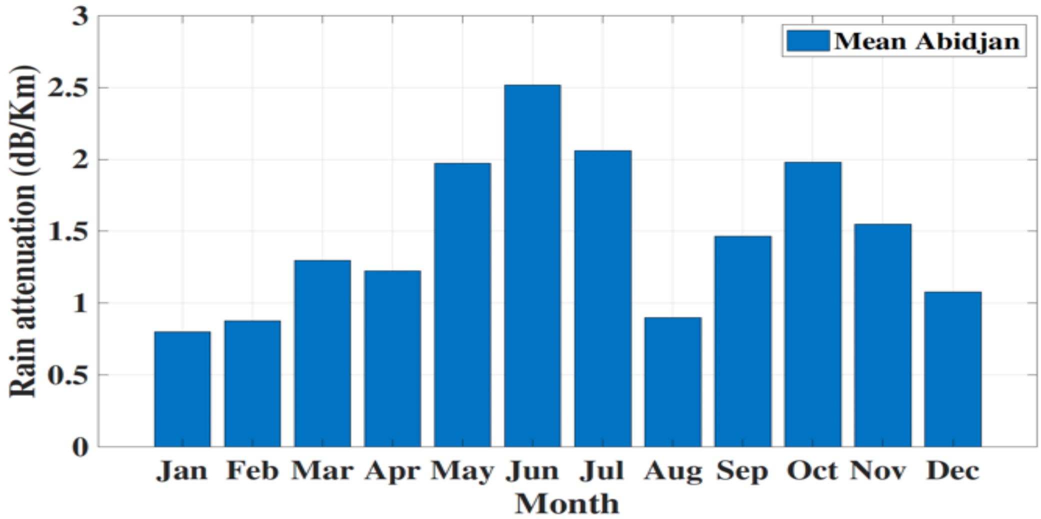

Figure II.16: *FSO link attenuation due to rain, depending on the month. [39]*

II.5.2.b Empirical Rain Attenuation Models

Several empirical models aim to predict rain attenuation for FSO links. A usual form for these models is given by:

$$Att_{rain} = k_1 R^{K_2} \tag{II.29}$$

Where Att_{rain} is the rain attenuation (dB/km), and R is the rainfall rate (mm/hr), and k_1 and k_2 are model parameters that depend on factors such as wavelength and raindrop size distribution and may vary geographically and with rain type [28] .

The value of R according to different rain conditions is shown in Table II.2

Precipitation R Values (mm/hr)	Light rain	Medium rain	Heavy rain	Cloud burst & heavy rain
Precipitation	2.5	12.5	25	100

Table II.2: *Precipitation R Values at different Rain Conditions*

The ITU-R (International Telecommunication Union - Radiocommunication Sector) provides models for rain attenuation, primarily developed for microwave and millimeter-wave frequencies. While these models are not directly applicable to optical frequencies due to the different scattering mechanisms and wavelength regimes, they serve as a basis for developing FSO-specific rain attenuation models. Some researchers have adopted these general principles to propose models specifically for FSO, using rainfall rate statistics or even visibility under rainy conditions as input parameters [48] [49].

II.5.3 Snow

Snowfall also impacts FSO links through scattering of the optical beam by snow particles. The attenuation caused by snow lies between that of rain and fog [35] [16].

II.5.3.a Types of Snow and Attenuation

Snow can be classified into wet and dry snow, with wet snow causing higher attenuation due to liquid water on snowflakes. Dry snow impacts link more at low snowfall rates, while wet snow impacts link more at high rates [29].

Figures 17-18 indicate an inverse relationship between snowfall visibility and attenuation, where greater visibility enables higher transmission bit rates. Snow significantly impairs FSO link connectivity, restricting viable operational distances to approximately 250 meters [42].

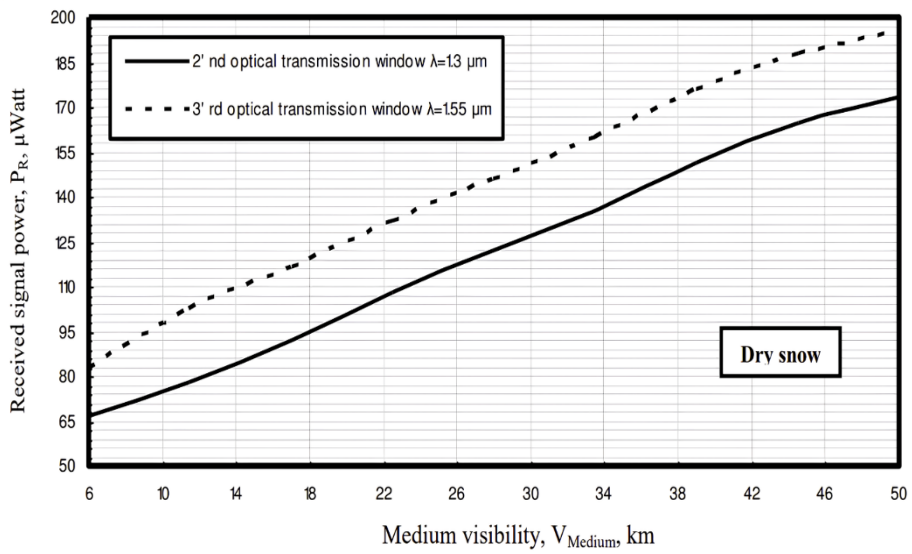

Figure II.17: *Received signal power in relation to medium visibility in Dry Snow. [42]*

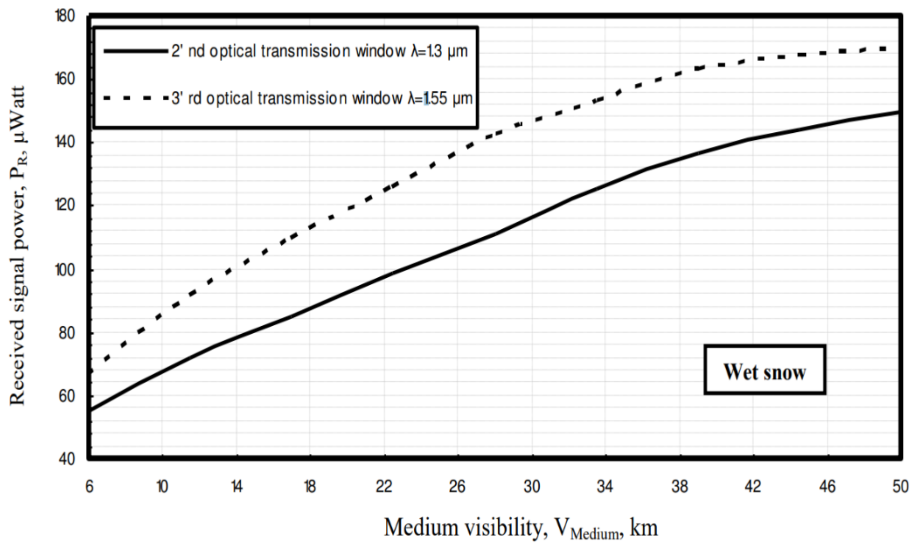

Figure II.18: *Received signal power in relation to medium visibility in Wet Snow. [42]*

II.5.4 Dust Storms

Dust storms are a significant atmospheric phenomenon in arid and semi-arid regions, notably in desert environments. These storms consist of fine particles suspended in the air, which scatter and absorb optical signals, leading to substantial attenuation in FSO communication links. The severity of attenuation depends on factors such as particle concentration, size distribution, and atmospheric visibility.

II.5.4.a Classification of Dust Storms and Attenuation

Dust storms can be categorized based on visibility ranges:

- **Severe Dust Storm**: Visibility < 0.2 km
- **Moderate Dust Storm**: Visibility between 0.2 km and 1 km
- **Blowing Dust**: Visibility between 1 km and 10 km
- **Dust Haze**: Visibility > 10 km

Attenuation due to dust storms is inversely related to visibility. For instance, at a visibility of 0.1 km, attenuation can reach up to 174 dB/km at a wavelength of 405 nm, while at 1550 nm, it is approximately 126 dB/km. This indicates that longer wavelengths experience less attenuation under identical conditions.

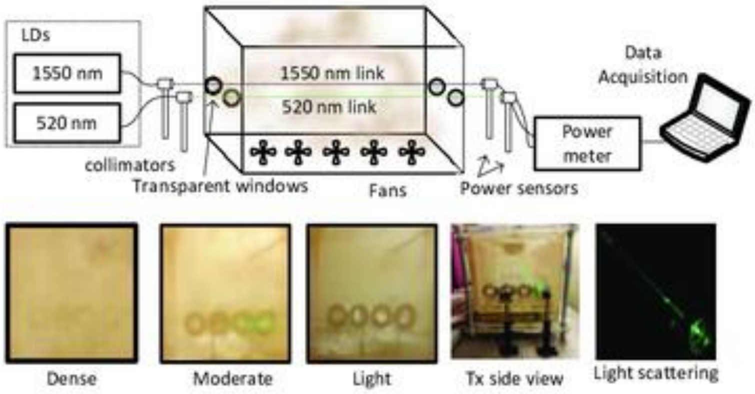

Figure II.19: *Experimental setup to measure dust effect on FSO links. [43]*

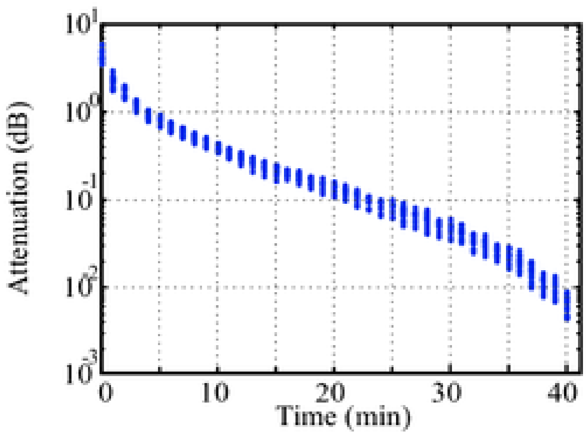

Figure II.20: *Attenuation (dB) against time. [43]*

II.5.5 Temperature Effects on FSO Attenuation

High ambient temperatures, characteristic of desert climates, influence FSO link performance by inducing atmospheric turbulence. This turbulence causes fluctuations in the refractive index, leading to beam wander, scintillation, and intensity fluctuations at the receiver. The strength of turbulence is quantified by the refractive index structure parameter C_n^2, which increases with temperature gradients.

Moreover, elevated temperatures can exacerbate the effects of dust storms by reducing air density, allowing dust particles to remain suspended longer, thereby prolonging attenuation effects. However, temperature alone, in the absence of particulates, has a lesser impact on attenuation compared to dust-induced scattering.

II.6 Conclusion

In summary, this chapter has established the fundamental principles governing free-space optical propagation, from the selection of transmission wavelengths within the near- and short-infrared bands to the behavior of Gaussian beams under diffraction and coherence constraints. We have examined how atmospheric phenomena absorption, scattering, turbulence, and weather events such as fog, rain, and snow introduce attenuation, scintillation, beam wander, and spreading, and seen how the Beer-Lambert law and statistical models (log-normal, Gamma-Gamma, K-distribution) quantify these impairments. Finally, we explored practical countermeasures optimal wavelength choice, beam-expander optics, polarization and spatial diversity, and adaptive protocols that together form a toolkit for enhancing link reliability. Armed with these theoretical insights and modeling frameworks, the design and optimization of robust FSO systems capable of high-speed, license-free wireless communication can proceed with greater confidence

General Conclusion

General Conclusion

The thesis investigates the performance of 10 Gb/s 16-QAM free-space optical communication systems in El Oued's desert environment. It develops a simulation model incorporating realistic attenuation profiles, providing valuable insights for network planners and engineers working in such challenging environments.

The systematic evaluation of three key wavelengths (850 nm, 1310 nm, and 1550 nm) revealed distinct performance characteristics under desert conditions. The 850 nm wavelength, while offering potential advantages in transmit power, demonstrated severe limitations due to pronounced Mie and Rayleigh scattering effects, becoming essentially unusable under moderate to severe dust conditions. The 1310 nm wavelength showed improved performance, offering a middle ground in terms of atmospheric penetration, yet still failed to meet reliability targets during peak storm conditions. In contrast, the 1550 nm configuration consistently outperformed the other wavelengths, maintaining Q-factors above the critical threshold ($Q > 6$) and bit error rates below 10^{-9} across nearly all tested scenarios.

The superior performance of 1550 nm systems can be attributed to several key factors. The longer wavelength experiences significantly reduced atmospheric scattering effects compared to shorter wavelengths, while also benefiting from mature optical amplification technologies (EDFAs) and higher permissible transmit power levels under eye safety regulations. These advantages make 1550 nm the clear choice for reliable FSO communication in desert environments. However, the research also identified important limitations - even 1550 nm systems face substantial challenges during extreme weather events, with severe dust storms and dense fog reducing effective communication ranges to just tens or hundreds of meters.

Future research should focus on developing intelligent hybrid FSO/RF networks with seamless switching algorithms and mm Wave backup links. Advanced adaptive systems, auto-alignment mechanisms, and improved transceiver designs can enhance resilience in desert environments. Field testing in actual desert conditions can validate these innovations and create more robust optical communication systems.

References

The References

[1] "Collaborative Robots Market," Variant Market Research, Report CR18129, Jul. 2017.

[2] H. Henniger and O. Wilfert, "An introduction to free-space optical communications," Journal of Radio Engineering, vol. 19, no. 2, pp. 203–212, Jun. 2010.

[3] "Picturing a Voice: Margaret Watts Hughes and the Eidophone," Brewminate, Apr. 30, 2025. [Online]. Available: https://brewminate.com/picturing-a-voice-margaret-watts-hughes-and-the-eidophone/. Accessed: Apr. 30, 2025.

[4] "fSONA unveils 2-5-Gbps free-space optical systems," Sep. 5, 2012.

[5] A. G. Alkholidi and K. S. Altowij, Free Space Optical Communications Theory and Practices. London, U.K.: IntechOpen, 2014.

[6] M. Beshr and M. H. Aly, "Outdoor wireless optical communication system attenuation at different weather conditions," International Journal of Optics, vol. 2015, Article ID 2015, 2015.

[7] F. Nadeem, V. Kvicera, M. S. Awan, E. Leitgeb, S. S. Muhammad, and G. Kandus, "Weather effects on hybrid FSO/RF communication link," IEEE Journal on Selected Areas in Communications, vol. 27, no. 9, pp. 1687–1697, Dec. 2009.

[8] "A scheme of FSO communication technology with optical wireless," ResearchGate. [Online].Available:https://www.researchgate.net/publication/309174268_Design_and_implementation_of_mobile_laser_data_transceiver. Accessed: Apr. 31, 2025.

[9] H. Kaushal, V. K. Jain, and S. Kar, "Applications of FSO communication systems," in Free Space Optical Communication, Springer, 2017, pp. 34–37.

[10] "FSO Backhaul Connectivity for Cellular Networks," ResearchGate. [Online]. Available: https://www.researchgate.net/publication/346556967_A_Contemporary_Survey_on_Free_Space_Optical_Communication_Potential_Technical_Challenges_Recent_Advances_and_Research_Direction. Accessed: Apr. 31, 2025.

[11] A. G. Alkholidi and K. S. Altowij, "Free space optical communications theory and practices," IntechOpen, Nov. 26, 2014.

[12] N. Hadjadji, "Contribution à l'étude des techniques et dispositifs dédiés aux réseaux de télécommunications optiques reconfigurables," Ph.D. dissertation, Univ. [Institution], Mar. 2, 2021.

[13] M. Singh and S. Gupta, "Multi-level pseudo-random sequence generation for coherent optical transmission systems," Jul. 4, 2014.

[14] N. Hadjadji, "Contribution à l'étude des techniques et dispositifs dédié," 2021.

[15] "Blue laser diodes," Laser Components, Apr. 31, 2025. [Online]. Available: https://www.lasercomponents.com/nordics/photonics-portal/news/blue-laser-diodes/.

Accessed: Apr. 31, 2025.

[16] M. H. Abu Jahid, A. Alsharif, and T. J. Hall, "A contemporary survey on free space optical communication: potentials, technical challenges, recent advances, and research direction," Apr. 2022.

[17] A. Abisayo, "Optically amplified free-space optical communication systems," Jul. 2013.

[18] R. Jee and S. Chandra, "WDM-FSO system for 5G wireless network using spatial multiplexing in the presence of wireless and optical nonlinearities," Sep. 25, 2024.

[19] L. F. B. Ribeiro, J. R. F. Da Rocha, and J. L. Pinto, "Performance evaluation of EDFA preamplified receivers taking into account intersymbol interference," Journal of Lightwave Technology, vol. 13, no. 2, pp. 225–232, Feb. 1995.

[20] M. Abtahi, P. Lemieux, W. Mathlouthi, and L. A. Rusch, "Suppression of turbulence-induced scintillation in free space optical communication systems using saturated optical amplifiers," Journal of Lightwave Technology, vol. 24, no. 12, pp. 4966–4973, Dec. 2006.

[21] X. Chen, C. Antonelli, A. Mecozzi, D. Di Che, and W. Shieh, "High-capacity direct detection systems," RP Photonics Encyclopedia.

[22] S. Babani, Y. S. Abdulmalik, A. Abdul'aziz, A. Z. Loko, and M. M. Gajibo, "Free space optical communication: The main challenges and its possible solution," International Journal of Scientific & Engineering Research, vol. 5, no. 7, Jul. 2014.

[23] H. Henniger and O. Wilfert, "An introduction to free-space optical communications," Radio Engineering, vol. 19, no. 2, Jun. 2010.

[24] L. Chaudhary, S. Yadav, and R. Mathur, "Next generation free space optics system in wireless communication technology," International Journal of Advances in Electrical and Electronics Engineering, no. 255.

[25] A. Vanderka et al., "Testing FSO WDM communication system in simulation software Optiwave OptiSystem in different atmospheric environments," VSB-Technical Univ. of Ostrava, Dept. of Telecommunications.

[26] K. Periyasamy et al., "A novel method for analyzing the performance of free space optical communication in WDM using EDFA," Proc. Inst. Elect. Eng., Aug. 1, 2022.

[27] H. Singh et al., "Designing an optimized free space optical (FSO) link for terrestrial commercial applications under turbulent channel conditions," Apr. 11, 2023.

[28] H. Khalil et al., "FSO communication: Benefits, challenges, and its analysis in DWDM communication system," Sir Syed Univ. Res. J. Eng. Technol., vol. –, no. –, Apr. 1, 2020.

[29] J. G. Chalil, S. Kadam, C. Joseph, K. J. Kulkarni, and A. A. B. Raj, "Characterization of free-space Gaussian beam propagation and recent developments of FSO communication technology: A review," Int. J. Eng. Res. Rev., vol. 12, no. 3, pp. 1–24, Jul.–Sep. 2024.

[30] M. Born and E. Wolf, Principles of Optics, 7th ed. Cambridge, U.K.: Cambridge Univ. Press, 1999.

[31] "Coherent and incoherent addition of waves," GeeksforGeeks, May 20, 2024. [Online]. Available:https://www.geeksforgeeks.org/coherent-and-incoherent-addition-of-waves/.Accessed: Mar. 16, 2025.

[32] R. Paschotta, "Coherence," RP Photonics Encyclopedia, Feb. 2025. [Online]. Available: https://www.rp-photonics.com/coherence.html. Accessed: Mar. 16, 2025.

[33] A. K. Rahman et al., "Impact of rain weather over free space optic communication," Proc. [Conference].

[34] "Ozone: Space Vision (Space monitoring of Earth Atmospheric Ozone)," ResearchGate. [Online].Available:https://www.researchgate.net/publication/291164378_Ozone_Space_Vision_Space_monitoring_of_Earth_Atmospheric_Ozone291164378_Ozone_Space_Vision_Space _monitoring_of_Earth_Atmospheric_Ozone. Accessed: May. 5, 2025.

[35] G. Yang, "Space-diversity free-space optical systems: performance analysis under correlated fading conditions," May 11, 2020.

[36] S. Kaur and A. Kakati, "Analysis of free space optics link performance considering the effect of different weather conditions and modulation formats for terrestrial communication," Apr. 30, 2018.

[37] "Harnessing polarization diversity for enhanced reliability in free space optical communications,"ResearchGate.[Online].Available:https://www.researchgate.net/publication/378901505_Harnessing_Polarization_Diversity_for_Enhanced_Reliability_in_Free_Space_Optical_Communications. Accessed: May. 5, 2025.

[38] A. Abisayo, "Optically amplified free-space optical communication systems," Jul. 2013.

[39] D. Kone, A. S. Penétjiligué, and A. Kamagaté, "Evaluation of free space optical (FSO) link under weather conditions in Abidjan," Int. J. Phys., Nov. 2024.

[40] E. Ebrahim and E. Bakery, "Design and analysis of DWDM transmission system for free space optical communications," in Faculty of Engineering, Mansoura Univ., 2018.

[41] A. El-Qady and M. Abaza, "Performance analysis of the effects of atmospheric turbulence on free space optical communication using multi-hop decode and forward relay in north and south of Egypt," Aug. 3, 2024.

[42] S. Chaudhary and A. Amphawan, "The role and challenges of free-space optical systems," Journal of Optical Communications, 2014.

[43]"An Experimental Study of FSO Link Performance in Desert Environment," ResearchGate.[Online].Available:https://www.researchgate.net/publication/304611997_An_Experimental_Study_of_FSO_Link_Performance_in_Desert_Environment.

Accessed: May 22, 2025.
[44] F. T. Mahmood, A. H. Ali, and A. H. A. Haeder, "Weather effect on the free space optics communication system," Indonesian Journal of Electrical Engineering and Computer Science, vol. 31, no. 1, pp. 222–228, Jul. 2023.
[45] A. Tou, S. Driz, B. Fassi, and I. S. K. Mahadjoubi, "Harnessing polarization diversity for enhanced reliability in free space optical communications," Mar. 6, 2024.
[46] N. A. Olsson, "Lightwave systems with optical amplifiers," Journal of Lightwave Technology, vol. 7, no. 7, pp. 1071–1082, Jul. 1989.
[47] C.-H. Liu, Y.-C. Chang, T. B. Norris, and Z. Zhong, "Graphene photodetectors with ultra-broadband and high responsivity at room temperature," Nature Nanotechnology, vol. 9, no. 4, pp. 273–278, Mar. 2014.
[48] E. Verdugo, L. d. S. Mello, C. P. Colvero, and R. Nebuloni, "Estimation of rain attenuation in FSO links based on visibility measurements," Mar. 2023.
[49] S. Magidi and T. Pondani, "Estimating the performance of free space optical communication in rain weather conditions using various models and modified duobinary return to zero technique," Sep. 10, 2020.
[50] N. Sliti and B. Mrabet, "Performance evaluation of free space optical communication under adverse weather conditions in desert environments using OptiSystem," Int. J. Adv. Comput. Sci. Appl., vol. 14, no. 2, pp. 456–462, 2023.
[51] H. Fathallah, T. A. Eltaif, and M. H. Aly, "Effect of sandstorm on FSO link performance in Middle Eastern desert environment," Optics Communications, vol. 444, pp. 165–170, 2019.
[52] Z. Huang, Q. Li, and W. Shieh, "Self-coherent detection for turbulence-mitigation in free-space optical communications," Nature Communications, vol. 12, no. 1, Art. no. 1234, 2021.
[53] A. Ali, S. Iqbal, and M. Yousaf, "Performance analysis of hybrid FSO/RF communication system in dusty weather conditions," IEEE Access, vol. 11, pp. 33142–33152, 2023.

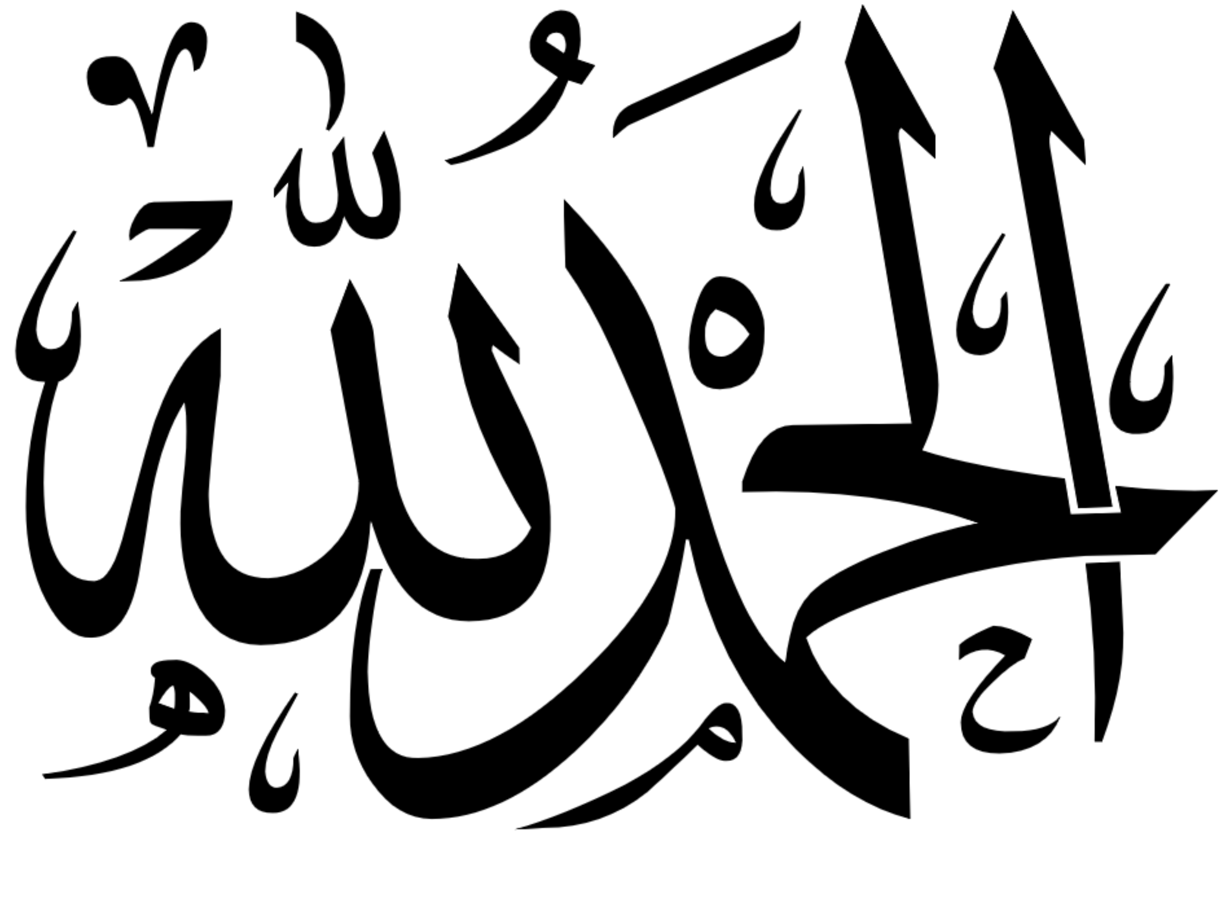
الحمد لله